A Simple Model of Nonlinear Hadley Circulation with an ITCZ: Analytic and Numerical Solutions

MING FANG AND KA KIT TUNG

Department of Applied Mathematics, University of Washington, Seattle, Washington

(Manuscript received 5 April 1995, in final form 23 August 1995)

ABSTRACT

Simple analytic solutions are constructed for an axially symmetric, nonlinear, slightly viscous circulation in a Boussinesq atmosphere in the presence of intense convection at an intertropical convergence zone. The latitude–height extent of the Hadley circulation is obtained, as well as its streamfunction, zonal wind, and temperature distribution. Numerical solutions of the viscous primitive equations are also obtained to verify the analytic solutions. The strength of the circulation is stronger than previous results based on dry models and is now close to the observed value. The extent of the Hadley region is also quite realistic.

1. Introduction

From the late 1970s, a series of studies (Schneider and Lindzen 1977; Schneider 1977; Held and Hou 1980; Lindzen and Hou 1988; Hou and Lindzen 1992; Plumb and Hou 1992) advanced our understanding of the dynamics of the Hadley circulation in the absence of eddies. In these studies, many features of the Hadley circulation, such as its meridional extent, flat horizontal temperature gradient, angular momentum conservation, and the intensification of the winter circulation cell have been explored.

Schneider (1977) noted that the nonlinear advection of angular momentum is important and the absolute angular momentum is conserved if friction is negligible. Held and Hou (1980), Lindzen and Hou (1988), and Hou and Lindzen (1992) developed a simple approximate theory using the concept of angular momentum conservation. In these studies, all thermal forcing are idealized by a simple Newtonian cooling processes: $Q = (T_E - T)/\tau$, and frictional processes are parameterized by viscous diffusion. Hereafter, we will refer to these models as Newtonian cooling models (NC models). The physical interpretation of T_E is the temperature at equilibrium in the absence of large-scale meridional circulation. In this formulation, T_E can be viewed as the consequence of the local convective-radiative equilibrium in the Tropics. When a large-scale circulation (the Hadley circulation) is present, the temperature T in the NC models differs from its equilibrium state T_E in the region of the circulation.

It is well known that moisture convergence and latent heat release in the intertropical convergence zone (ITCZ) play an important role in the dynamics of the Hadley circulation (Riehl and Malkus 1958). There have been attempts to incorporate latent heating in the NC models by simply changing the specification of T_E in an otherwise dry model. For example, Hou and Lindzen (1992) used a latitudinally concentrated T_E to include the effect of a concentrated latent heating in the ITCZ.

Although one could include some effects of moist convection this way, for example, by defining T_E to be that obtained under convective–radiative equilibrium instead of the value obtained under radiative equilibrium, there is a fundamental conceptual difference between a moist convecting and a dry atmosphere in the way temperature adjustment is accomplished, which has only recently been clarified (see Emanuel et al. 1994; Yanai et al. 1973; Cane and Sarachik 1989). Since cumulus convective adjustment is probably a much faster process, the local temperature in regions of active convection should be nearly in convective-radiative equilibrium—that is, $T \approx T_E$. The effect of the large-scale circulation on T is of second order and affects mainly the conditions for convection (e.g., the availability of moisture convergence) and to a less extent the lower-level temperature in the subcloud layer (Emanuel et al. 1994). In other words, the temperature profile itself, rather than the net heating, is controlled by convection. Such a conceptual change in the way we view the relationship between temperature and heating actually results in considerable simplification in theoretical models of Hadley circulation.

Corresponding author address: Dr. Ka Kit Tung, Department of Applied Mathematics, University of Washington, Box 35420, 408 Guggenheim Hall, Seattle, WA 98195.

Confirmation of this conceptual model can sometimes be found in numerical models incorporating moist convection. Satoh (1994) constructed a more consistent model by including the hydrological cycle and a radiation–convection scheme in his axisymmetric model. His results show that the vertical temperature profile in the strong rising region of the Hadley circulation is determined by local moist processes. It decreases from the sea surface temperature upward in such a way that the profile follows the moist adiabatic lapse rate. This vertical profile of temperature in the moist convective region is consistent with results from one-dimensional convective models (Sarachik 1978; Satoh and Hayashi 1992). The temperature is almost flat latitudinally inside the Hadley circulation cell. Outside the circulation cell, the temperature depends on the surface temperature and is determined by the local radiative equilibrium.

Satoh's results also show that the upper-level poleward flow conserves angular momentum, and zonal wind and vertically averaged temperature are in cyclostrophic balance. Satoh's numerical work provides the motivation for our present attempt at constructing a simple analytic solution to the problem. Satoh (1994) also tried to obtain some analytic results on some averaged quantities, such as the total poleward mass flux, and the extent of the Hadley circulation at the top and the bottom of his model, making additional simplifying assumptions not justified by his numerical results. In addition, the two-dimensional (meridional-height) structure of the circulation and the detail of the meridional velocity and the vertical velocity have not been fully explored. Our analytic solutions are a result of asymptotic deduction and provide a detailed meridional-height distribution of the meridional circulation, temperature, zonal wind, and the separation curve between the circulation region and the equilibrium region. Our numerical solutions illustrate how viscosity affects the extent of the Hadley circulation and the total mass flux.

In this paper, we propose a simple physically consistent model to describe the Hadley circulation in a convective axisymmetric atmosphere. In this model, the ITCZ is idealized as an extremely narrow band centered at one latitude, not necessarily symmetric about the equator. The vertical temperature profile in the ITCZ is determined by fast moist convection (and so is provided by a one-dimensional cumulus convection model or simply given by a moist adiabat), and the net heating at the ITCZ is determined by the resulting large-scale circulation as part of the solution. This model provides an alternative approach that differs from the earlier NC models, in which the latent heating is specified, and the temperature and circulation are resulting solutions. Away from the ITCZ, the diabatic heating (cooling) in our model is still approximated by a Newtonian cooling form as in the NC models. Under the assumption of small viscosity and long Newtonian cooling time away from the ITCZ, angular momentum conservation, cyclostrophic balance, and hydrostatic balance can be shown to hold asymptotically away from the ITCZ. This model turns out to be even simpler than the NC model, and an analytic solution in the "nearly inviscid limit" is obtainable. In section 2, we describe the formulation of our model. Some general features of the solution in the nearly inviscid limit are discussed in section 3. Analytic solutions are obtained in section 4. The examples for both equatorially symmetric and asymmetric equilibrium temperatures are shown in section 5. The solutions are verified by numerical solutions presented in section 6. Concluding remarks follow in section 7. Some cases not given analytic solutions in section 3 are discussed in the appendix.

2. The model

a. The primitive equations

In this simple model, we consider a set of steady, axially symmetric primitive equations for a Boussinesq fluid on a sphere of radius a rotating with rate Ω, confined between the bottom solid surface and a stress-free lid at height H. Let T be the temperature, T_0 the constant of globally averaged temperature, Q the diabatic heating rate per unit mass, and (u, v, w) the velocity of the fluid in the longitudinal, latitudinal (ϕ), and the vertical (z) direction, respectively. The equations are

$$\frac{\partial u}{\partial t} + \frac{v}{a}\frac{\partial u}{\partial \phi} + w\frac{\partial u}{\partial z} - \frac{uv}{a}\tan\phi - 2\Omega v\sin\phi = \nu\nabla^2 u \quad (1)$$

$$\frac{\partial v}{\partial t} + \frac{v}{a}\frac{\partial v}{\partial \phi} + w\frac{\partial v}{\partial z} + \frac{u^2}{a}\tan\phi + 2\Omega u\sin\phi = \nu\nabla^2 v - \frac{1}{a}\frac{\partial \Phi}{\partial \phi} \quad (2)$$

$$\frac{1}{a}\frac{\partial (v\cos\phi)}{\partial \phi} + \frac{\partial w}{\partial z} = 0 \quad (3)$$

$$\frac{\partial \Phi}{\partial z} = g\frac{T}{T_0} \quad (4)$$

$$\frac{\partial T}{\partial t} + \frac{v}{a}\frac{\partial T}{\partial \phi} + w\left(\frac{\partial T}{\partial z} + \Gamma_d\right) = \kappa\nabla^2 T + \frac{Q}{C_p}, \quad (5)$$

where Γ_d is the dry adiabatic lapse rate and C_p is the specific heat of the gas at constant pressure. To calculate the steady-state solution analytically, we drop the time derivative terms in Eqs. (1)–(5). The numerical solutions presented in section 6 use time stepping and so need the full time-dependent equations.

b. Heating

Suppose that the diabatic heating can be approximated by the Newtonian cooling law as in Schneider (1977):

$$\frac{Q}{C_p} = \frac{T_E - T}{\tau(\mu)}, \tag{6}$$

where $\mu \equiv \sin\phi$, T_E is the equilibrium temperature and τ is the relaxation time.[1] Suppose a convection region is centered at latitude μ_1. Since the local convection process is much faster than the large-scale circulation, we can incorporate this process in the form (6) by assuming $\tau(\mu) \to 0$ as $\mu \to \mu_1$ so that the temperature at μ_1 approaches T_E, the temperature at "*convective*-radiative equilibrium." This T_E can be found using a detailed one-dimensional model incorporating latent heating and radiation. An important characteristic of T_E found by most such models is that its lapse rate is determined approximately by a moist adiabat; that is,

$$T(\mu_1, z) \to T_E(\mu_1, z) = T_M(z) \equiv T_{M0} - \Gamma_m z, \tag{7}$$

where Γ_m is the moist adiabatic lapse rate at μ_1. The ITCZ is considered as a very narrow band so that it is approximated by a single latitude μ_1. Away from this latitude, the diabatic heating is approximated by a slow Newtonian cooling process with $\tau(\mu) = \tau_0$, where τ_0 is a long constant relaxation time ($\sim$20 days). The surface temperature at μ_1, T_{M0}, is known to be determined mainly by the sea surface temperature, and to a minor extent by the large-scale circulation (see Emanuel et al. 1994). This latter dependence is ignored in present work and so $T_{M0} = T_s(\mu_1)$, where $T_s(\mu)$ is the locally specified surface temperature. Although we will use the simple form (7) in our examples discussed later, our model can alternatively incorporate a T_E calculated using a more detailed one-dimensional moist model as input.

The magnitude of the net heating Q and hence the vertical velocity at the ITCZ in this model depends on the ratio $(T_E - T)/\tau$, as the numerator and denominator each goes to zero. If $T \to T_E$ faster than $\tau \to 0$, there will be no heating, as the temperature adjusts rapidly to the local convective equilibrium. Otherwise there will be finite or even infinite heating. We allow for the latter possibility because T may approach T_E slower than $\tau \to 0$ at μ_1. The magnitude of the heating at the ITCZ is to be determined as part of the solution by the large-scale circulation. We therefore write for our model

$$\frac{Q}{C_p} = \frac{T - T_E}{\tau_0} + q(z)\delta(\mu - \mu_1), \tag{8}$$

where $q(z)$ is to be determined by mass conservation for the large-scale circulation. The delta function distribution is necessary to allow for the possibility of *finite* heating integrated over the ITCZ. If $q = 0$, the ITCZ will contribute no net heating. In any case,

$$T(\mu, z) \to T_E(\mu_1, z), \quad \text{as} \quad \mu \to \mu_1, \tag{9}$$

and so is known without a knowledge of the large-scale (Hadley) circulation. The highly idealized delta function heating form (8) was also adopted by Schneider (1983) in his modeling of Martian great dust storms. But in his parameterization, q, the strength of heat source, is related to dust/solar absorption and is specified, while in our model $q(z)$ is part of the solution. It is determined by the amount of sinking that occurs elsewhere in the circulation region.

c. Boundary conditions

The boundary conditions for the velocities are no-slip conditions at the bottom and stress-free lid at the top. The boundary is considered to be insulated so that no heat flux crosses it. There is no poleward velocity—that is, $v\cos\phi = 0$—at the poles.

d. Nondimensionalization

As in Fang and Tung (1994), nondimensional variables are introduced by asterisks as follows: $z^* = z/H$, $\tau^* = 2\Omega\tau$, $(u^*, v^*) = (u, v)/U$, $w^* = (w/U)(a/H)$, $\Phi^* = \Phi/2\Omega aU$, $\nabla^{*2} = H^2\nabla^2$, and

$$T^* = \frac{T}{T_0}\frac{gH}{2\Omega aU} = \frac{R_H}{\mathrm{Ro}}\frac{T}{T_0}.$$

Here U is a typical zonal velocity, $\mathrm{Ro} \equiv U/(2\Omega a)$ is Rossby number, and $R_H \equiv gH/(2\Omega a)^2$. After the nondimensionalization process, the superscript asterisks for the nondimensional variables are dropped without confusion. The following nondimensional fundamental steady-state equations are obtained:

$$\mathrm{Ro}\left(v\frac{\partial u}{\partial\phi} + w\frac{\partial u}{\partial z} - uv\tan\phi\right) - \sin\phi v = E\nabla^2 u \tag{10}$$

$$\mathrm{Ro}\left(v\frac{\partial v}{\partial\phi} + w\frac{\partial v}{\partial z} + u^2\tan\phi\right) + \sin\phi u = E\nabla^2 v - \frac{\partial\Phi}{\partial\phi} \tag{11}$$

$$\frac{\partial(v\cos\phi)}{\partial\phi} + \frac{\partial w}{\partial z} = 0 \tag{12}$$

$$\frac{\partial\Phi}{\partial z} = T. \tag{13}$$

[1] More precisely, T_E is the temperature at equilibrium obtained in the absence of the large-scale meridional circulation. It can be obtained by a one-dimensional model that treats the atmosphere locally, column by column, to be in radiative–convective equilibrium, as in, for example, Sarachik (1978) and Satoh and Hayashi (1982).

At μ_1, the temperature is from (7)

$$T(\mu_1, z) = T_M(z) \equiv T_{M0} - \delta_m z, \qquad (14)$$

and away from μ_1, we have $\tau = \tau_0$ and

$$\mathrm{Ro}\left(v\frac{\partial T}{\partial \phi} + w\frac{\partial T}{\partial z} + \delta_d w\right) = \frac{E}{\sigma}\nabla^2 T + \frac{T_E - T}{\tau_0}, \qquad (15)$$

where $E \equiv \nu/(2\Omega H^2)$ is Ekman number, and $\sigma \equiv \nu/\kappa$ is Prandtl number. Additionally, $\delta_d \equiv \Gamma_d H R_H/(\mathrm{Ro} T_0)$ is the nondimensional dry adiabatic lapse rate and $\delta_m \equiv \Gamma_m H R_H/(\mathrm{Ro} T_0)$ is the nondimensional moist lapse rate.

The parameter regime relevant to the real atmosphere is

$$E \ll 1, \quad \tau_0 \gg 1, \quad \text{and} \quad E\tau_0 \ll 1.$$

For a dimensional Newtonian relaxation time of 20 days, we find

$$\tau_0 \approx 250 \gg 1.$$

For a typical kinematic viscosity coefficient of $\nu = 5$ $\mathrm{m^2\ s^{-1}}$, we have

$$E \approx 10^{-4} \ll 1,$$

where we have taken $H = 15$ km as the height of the "tropopause." The product yields

$$E\tau_0 \approx 0.025 \ll 1.$$

The condition, $E\tau_0 \ll 1$, defines the "nearly inviscid limit" in the present work.

The Prandtl number σ is taken to be order one or larger. The value of the Rossby number, Ro, is mostly not restricted[2] in the present work, except that the case of $\mathrm{Ro} < 80E^2$ has been dealt with separately in Fang and Tung (1994), where exact solutions were found. The work presented here assumes that $\mathrm{Ro} > 80E^2$. For the terrestrial atmosphere Ro = 0.03 is small, but is still larger than $80E^2$.

e. Occurrence of Hadley circulation

In general, a Hadley circulation will occur, with or without moist convection, whenever there is a meridional gradient of the equilibrium temperature T_E at the equator. Only under very restricted conditions [$E \to 0$, $\partial T_E/\partial\mu = 0$, $\partial^2 T_E/\partial\mu^2 = 0$ at $\mu = 0$ and Ro small enough (see Fang and Tung 1994)] can the atmosphere relax to the radiative–convective equilibrium with $(v, w) = (0, 0)$ over the globe. For the case $E \to 0^+$, $\partial T_E/\partial\mu = 0$ but $\partial^2 T_E/\partial\mu^2 \neq 0$ at $\mu = 0$, the equilibrium solution, although it exists, is unstable to symmetric inertial instability in the purely inviscid limit, and, in the "nearly inviscid" limit (E small, but nonzero), it is incompatible with the presence of viscosity, no matter how small it is (Hide's theorem, see Held and Hou 1980). So even in this case, a Hadley circulation exists, at least near the equator.

3. Some general results

There are some very simple but rather general results that can be shown to be valid for axisymmetric circulations with or without convection. The most important of these is the result on *latitudinal temperature homogenization,* which has previously be noted in numerical results in dry (Held and Hou 1980; Lindzen and Hou 1988) as well as moist (Satoh 1994) model atmosphere. These general results will first be derived here, along with conditions for their validity, as part of the leading order asymptotic solution of the primitive equations. Specializing to our case in the presence of an ITCZ will be done in section 4.

a. Angular momentum conservation

In the "nearly inviscid limit," defined by $E\tau_0$ small, absolute angular momentum in the zonal direction is conserved along streamlines away from thin viscous boundary layers and the ITCZ.

Away from the ITCZ, and for $E \to 0^+$, one can show from Eq. (12) that (v, w) are proportional to Q and therefore are scaled by $1/\tau_0$. We can rescale them by introducing $v = \hat{v}/\tau_0$, $w = \hat{w}/\tau_0$. Thus, the angular momentum Eq. (7) can be rewritten as

$$\mathrm{Ro}\left(\hat{v}\frac{\partial u}{\partial \phi} + \hat{w}\frac{\partial u}{\partial z} - u\hat{v}\tan\phi\right) - \sin\phi\hat{v} = E\tau_0\frac{\partial^2 u}{\partial z^2}. \qquad (16)$$

Thus, it can be seen that if $E\tau_0 \ll 1$, the absolute angular momentum is conserved along streamlines away from viscous boundary layers; that is,

$$\hat{v}\frac{\partial L}{\partial \phi} + \hat{w}\frac{\partial L}{\partial z} = 0 \quad \text{for} \quad E\tau_0 \ll 1, \qquad (17)$$

where $L \equiv \cos^2\phi + 2\,\mathrm{Ro} u\cos\phi$ is the absolute angular momentum.

In the current problem, there is a viscous boundary layer near the lower boundary, and an "inner viscous layer" near the meridional edge of the Hadley circulation region. In these regions, absolute angular momentum conservation may not hold.

There are two possible solutions to Eq. (17) away from these boundary layers: one is an equilibrium solution with no circulation [i.e., $(v, w) \equiv 0$], and the other is a statement of conservation of absolute angular

[2] In the boundary layer asymptotic analysis presented in section 5, the nature of the viscous and thermal diffusive boundary layers is different dependent on whether Ro is small or not. Only the case of small Ro is worked out in detail in that example.

momentum conservation: $L = L(\Psi)$ where $(v, w) \neq 0$, with Ψ being the streamfunction for (v, w), $v \cos\phi = -\partial\Psi/\partial z$, $w = \partial\Psi/\partial\mu$. In most relevant cases, the equilibrium solution $(v, w) = 0$ can be ruled out for one reason or the other (see the discussion at the end of section 2). In these cases we are then left with the only solution

$$L = L(\Psi), \tag{18}$$

which, incidently, includes the relevant case of nonzero circulation in some region in the Tropics, and no circulation in the extratropics near the poles.

In the purely inviscid case, the functional form for L is nonunique, being determined presumably by the initial conditions. In the slightly viscous (or sometimes called the "nearly inviscid") case (E small but nonzero), absolute angular momentum, as well as other conserved quantity, should be homogenized inside closed streamlines at steady state, a result first stated by Batchelor (1956), and later expressed as Hide's theorem by Schneider (1977) and Held and Hou (1980). Since the real atmosphere is never in a steady state, it is not clear which limit is the more appropriate one. This issue will be left to a future paper on time-dependent Hadley circulations. Here we shall pursue the slightly viscous steady-state limit further.

In such a limit, the solution to (18) in the Hadley circulation region is

$$L = L_0, \quad \text{a constant},$$

or, stated in another way,

$$u = \frac{\mu^2 - \mu_S^2}{2\,\mathrm{Ro}(1 - \mu^2)^{1/2}}, \tag{19}$$

where μ_S is the stagnation point where $u = 0$, which yields $L_0 = 1 - \mu_S^2$. At this stage we have not yet determined where μ_S is.

b. Cyclostrophic balance

It is often assumed that geostrophy (or cyclostrophic balance in the nonlinear case) holds for large-scale nearly inviscid flows away from the equator. To these conditions one must add the additional constraint that the timescale of temperature adjustment must be long—that is, $\tau_0 \gg 1$. Consequently, cyclostrophic balance does not hold inside an ITCZ and in other regions of intense convection, nor in a viscous boundary layer. It will not be invoked in the present work in these regions.

The meridional momentum equation (11) can be rewritten as

$$\frac{\mathrm{Ro}}{\tau_0^2}\left(\hat{v}\frac{\partial\hat{v}}{\partial\phi} + \hat{w}\frac{\partial\hat{v}}{\partial z}\right) + \mathrm{Ro}u^2\tan\phi + \sin\phi u = \frac{E}{\tau_0}\frac{\partial^2\hat{v}}{\partial z^2} - \frac{\partial\Phi}{\partial\phi}. \tag{20}$$

For $\tau_0 \gg 1$, (20) reduces to a statement about cyclostrophic balance:

$$\mathrm{Ro}u^2\tan\phi + \sin\phi u = -\frac{\partial\Phi}{\partial\phi}. \tag{21}$$

Remarkably, cyclostrophic balance holds up to a thin region within

$$\mu \leqslant \sqrt{\mathrm{Ro}/\tau_0^2} \sim 7 \times 10^{-4}$$

of the equator for $\mathrm{Ro} \approx 0.03$ and $\tau_0 \approx 250$.

c. Latitudinal temperature homogenization

Combining cyclostrophic balance (21) with hydrostatic balance (13), we obtain the so-called thermal-wind relation:

$$\frac{\partial}{\partial z}(\mathrm{Ro}u^2\tan\phi + u\sin\phi) = -\frac{\partial T}{\partial\phi}. \tag{22}$$

In the Hadley circulation region, since u, given by (19), is a function of latitude only, the temperature must satisfy

$$\frac{\partial T}{\partial\phi} = 0. \tag{23}$$

In the nearly inviscid limit: $E\tau_0 \ll 1$, $\tau_0 \gg 1$, there is no horizontal temperature gradient in the Hadley circulation region, away from viscous boundary layers.

Thus, the effect of the Hadley circulation is to homogenize the temperature latitudinally within its core.

There may appear to be a technical difficulty in applying (23) across the equator because cyclostrophic balance (21) does not hold there. However, since the region where (21) may break down is thin meridionally, integrating (20) across the equator shows that Φ, and hence T, should be approximately continuous. Hence (23) holds even across the equator.

4. Analytic solution with an ITCZ

a. Temperature

As pointed out before, the result on latitudinal temperature homogenization, (21), was found by previous authors in numerical solutions for both the dry and moist models. In the dry NC models, the (latitudinally constant) temperature that the model attains in the Hadley circulation is determined by the so-called "equal-area rule" (Held and Hou 1980), so that the mass flux in the subsidence region, where $Q = (T_E - T)/\tau_0$ is negative, can balance the mass flux in the upwelling region, where Q is positive. Consequently, T thus determined is roughly halfway between the maximum T_E

and the minimum T_E found in the latitudes of the Hadley circulation region.

In the current model, when an intensive convection takes place in an ITCZ located at μ_1, and where the "statistical equilibrium" (Emanuel et al. 1994) holds, the temperature there is locally determined by the moist processes. We have, from (7),

$$T(\mu_1, z) = T_E(\mu_1, z) = T_M(z) \equiv T_{M0} - \delta_m z.$$

Combining this with the fact that $T(\mu, z)$ is independent of latitude inside the circulation region, we have, for the whole region inside the core of the Hadley circulation

$$T(\mu, z) = T(\mu_1, z) = T_E(\mu_1, z) = T_M(z) \equiv T_{M0} - \delta_m z. \quad (24)$$

The temperature in the Hadley region is completely and explicitly determined.

The physical consequence of (24) is that since the ITCZ usually occurs near where the tropical sea surface temperature is the warmest (assuming that there is enough moisture convergence), the temperature attained in the core of the Hadley circulation has the same, warmer value. Thus T in the Tropics in the model with an ITCZ is usually warmer than the T in the dry NC models. Consequently, the region of subsidence is wider and downward mass flux is greater in the current model than in previous dry NC models. This radiatively determined downward mass flux forces a low-level mass convergence into the ITCZ, producing an upwelling as a result. This Hadley mass flux thus produced is usually stronger than in dry models.

Contrary to common perceptions, the new conceptual model requires one to think of net heating and upwelling at the ITCZ not as a direct result of local latent heat release by the convection, but as a result of forced ascent by remote radiative-cooling-induced subsidence. Of course, the magnitude of subsidence is a function of the global temperature distribution in the Hadley cell. Latent heat release raises the local temperature at μ_1, which is then homogenized by the Hadley circulation to latitudes away from μ_1.

A corollary of (24) is that the vertical lapse rate in the Hadley circulation is approximately the same at all latitudes and follows approximately the moist adiabat appropriate for the latitude of the ITCZ.

This is also consistent with the numerical result of Satoh (1994), who found "the vertical temperature profile in the upward motion region of the Hadley circulation is determined by the moist process to be a moist adiabat, and the profiles in the downward motion have the same moist adiabat."

b. Geopotential

If $\tau_0 \gg 1$, the cyclostrophic balance, (22), is valid, except possibly in the thin viscous boundary layers. Note that the left-hand side of (21) can be written as

$$\mathrm{Ro}u^2 \tan\phi + u \sin\phi \equiv \frac{\partial}{\partial\phi}(\mathrm{Ro}u^2/2) - \frac{u}{2}\frac{\partial L}{\partial\mu}$$

since L is constant within the circulation region. Since there is a strong vertical motion carrying the absolute angular momentum all the way to the top in the ITCZ, we know the stagnation point, μ_S, should be in the same location of the ITCZ, that is, $\mu_S = \mu_1$. Integrating the cyclostrophic balance equation (21) from μ_1 to μ gives

$$\Phi(\mu, z) = \Phi_1(z) - \mathrm{Ro}u^2/2 \quad (25)$$

if the integration path is entirely within the circulation cell (angular momentum conserving region where $\partial L/\partial\mu = 0$). Here, $\Phi_1(z)$ is the geopotential profile at the latitude μ_1, where $u = 0$—that is, $\Phi_1(z) \equiv \Phi(\mu_1, z)$. Equation (25) gives the relationship between the geopotentials at two points in a horizontal line within the angular momentum conserving region. If the whole vertical line $\mu = \mu_1$ is in the circulation cell, the geopotential in the entire circulation region is given by (25).

c. Meridional circulation

In the circulation region, the vertical velocity at latitudes other than μ_1 can be obtained by combining (15) and (24) to yield

$$w = \frac{T_E - T_M}{\delta_s \tau_0 \mathrm{Ro}}, \quad \mu \neq \mu_1. \quad (26)$$

[Note that since T is independent of μ, the $v(\partial T/\partial\phi)$ term in (15) vanishes in the circulation region.] Here, $\delta_s \equiv \delta_d - \delta_m$ is a nondimensional static stability. The vertical velocity at μ_1 is determined by mass conservation. From (8), we know that w can also be written as

$$\mathrm{Ro}\delta_s w(\mu, z) = q(z)\delta(\mu - \mu_1) + \frac{T_E - T}{\tau_0}. \quad (27)$$

Based on the mass conservation requirement [derivable from (12)]

$$\int_{-1}^{1} w(\mu, z)d\mu = 0, \quad (28)$$

we obtain, for the magnitude of net heating at the ITCZ,

$$q(z) = -\int_{-1}^{1} \frac{T_E - T_M}{\tau_0} d\mu. \quad (29)$$

It is seen that it is equal to the total downward mass flux due to radiative cooling away from the ITCZ.

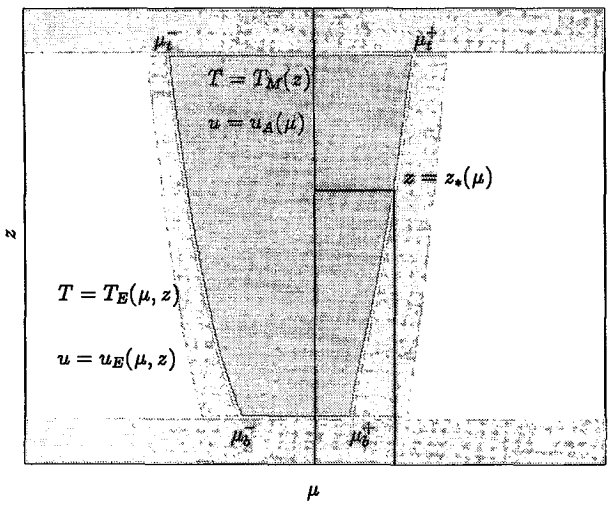

FIG. 1. Schematic structure of the Hadley circulation and its boundaries (see text).

Thus, net heating in the ITCZ is not locally determined but is a result of the large-scale subsidence elsewhere in the Hadley circulation region. Outside the circulation region, there is no meridional circulation and $T \approx T_E$.

In the NC models (e.g., Held and Hou 1980; Lindzen and Hou 1988), mass is required to balance in the Hadley circulation in the absence of an ITCZ by the so-called equal-area rule (Held and Hou 1980; Lindzen and Hou 1988). This temperature is usually colder than the T_M in our model. Consequently, the large-scale Hadley circulation is weaker than that in our model. The circulation strengths in the two models become nearly equal to each other if in our model we change T_M to be the calculated temperature profile from Held and Hou (1980) so that $q(z) \approx 0$ in (29).

d. Equilibrium zonal wind

As an example, we use the same T_E distribution for $\mu \neq \mu_1$ as in Held and Hou (1980), Lindzen and Hou (1988), and Satoh (1994):

$$\frac{T_E}{T_0} = T_{00} - \Delta_H(\mu - \mu_0)^2 - \Delta_V \frac{z}{H}, \qquad (30)$$

where $\Delta_V \equiv \Gamma H/T_0$ and Γ is the lapse rate of T_E. The nondimensional form is

$$T_E = \frac{R_H}{\mathrm{Ro}}[T_{00} - \Delta_H(\mu - \mu_0)^2 - \Delta_V z]. \qquad (31)$$

The equilibrium zonal wind can be obtained from (22) with $T = T_E$ and $u = 0$ at $z = 0$:

$$u_E = \frac{\sqrt{1-\mu^2}}{2\,\mathrm{Ro}}\left(\sqrt{1 + 8Rz\frac{\mu - \mu_0}{\mu}} - 1\right), \qquad (32)$$

where $R \equiv R_H\Delta_H$ can be considered as a thermal Rossby number.[3] It is noted that the equilibrium zonal wind does not exist in the region where

$$0 \leq \mu \leq 8R\mu_0 z/(1 + 8Rz).$$

Therefore, a Hadley circulation will at least occupy this region. The actual Hadley circulation region may be larger.

e. Boundary of the circulation region

Suppose in the nearly inviscid limit, the viscous effect is confined in narrow viscous boundary layers only (the scale of these boundary layers shrinks to zero as $\nu \to 0^+$). The meridional plane is mainly divided into two regions: the angular momentum conserving region and the equilibrium region, separated by a line $z = z_*(\mu)$ or $\mu = \mu_*(z)$. There may be a thin boundary layer (of thickness $\sim \sqrt{E\tau_0}$) around the separation line connecting all variables smoothly to each side. For small but nonzero viscosity there is also a viscous boundary layer near the lower and upper boundaries. The circulation pattern is schematically depicted in Fig. 1. The dark shaded area is the inviscid core of the circulation region where the zonal wind is given by (19) and the temperature is given by (24). The light shades area is the viscous boundary layer. Outside the shaded area is the equilibrium region where $T = T_E$ and the zonal wind is given by (32).

Now, we shall determine the boundaries of the Hadley circulation region. From (13), we have

$$\Phi(\mu, z_*) = \Phi_0(\mu) + \int_0^{z_*} T(\mu, z')dz'$$

$$= \Phi_0(\mu) + \int_0^{z_*} T_E(\mu, z')dz', \qquad (33)$$

where $\Phi_0(\mu)$ is the geopotential at the lower surface. On the other hand, suppose the path from μ_1 to μ at $z = z_*$ is in the circulation region, then from (25)

$$\Phi(\mu, z_*) = \Phi_1(z_*) - \frac{\mathrm{Ro}}{2}u^2. \qquad (34)$$

The continuity of the geopotential across the separation line leads to the following equation:

$$\Phi_0(\mu) + \int_0^{z_*} T_E(\mu, z')dz' = \Phi_1(z_*) - \frac{\mathrm{Ro}}{2}u^2. \qquad (35)$$

[3] The definition of R here is one-quarter of that in the definition of Held and Hou (1980).

Note

$$T(\mu_1, z) = T_M(z)$$

and

$$\Phi_1(z_*) \equiv \Phi(\mu_1, z_*) = \Phi_0(\mu_1) + \int_0^{z_*} T_M(z')dz'.$$

Substituting these expressions and (19) into (35), we have

$$\int_0^{z_*} (T_E - T_M)dz' = \Phi_0(\mu_1) - \Phi_0(\mu) - \frac{(\mu^2 - \mu_1^2)^2}{8\,\mathrm{Ro}(1 - \mu^2)}. \quad (36)$$

Thus, if we know μ_1 and the geopotential distribution at the bottom boundary, we can obtain the separation line from (36). The geopotential variation at the bottom boundary is due to the effect of viscosity. Before we discuss that, it should be pointed out that (36) should strictly be obtained with quantities evaluated above the bottom viscous boundary layer. In particular, the lower limit of the Φ integral in (36) should be d, the thickness of the boundary. However, since

$$\int_d^{z_*} (T_E - T_M)dz' = \int_0^{z_*} (T_E - T_M)dz' + O(E), \quad (37)$$

the difference is ignored. Similarly, the geopotentials on the right-hand side of (36) should also be evaluated at $z = d$ instead of $z = 0$, but the difference is generally ignored in boundary-type asymptotic calculation.

Evaluating the meridional momentum equation (11) at $z = 0$ and applying the no-slip boundary conditions, we find

$$\frac{\partial \Phi_0}{\partial \phi} = E \left.\frac{\partial^2 v}{\partial z^2}\right|_{z=0}. \quad (38)$$

Outside the Hadley circulation region—that is, $\mu > \mu_b^+$ or $\mu < \mu_b^-$, where μ_b^+ and μ_b^- are the northern and southern extent of the Hadley circulation region, respectively—the atmosphere is in radiative equilibrium except for the viscosity induced flow in the boundary layers at the lower and upper boundaries. The viscous problem in this region can be cast in the form of a Charney (1973) problem. Its analytic solution was obtained previously by Fang and Tung (1994) to be

$$E \left.\frac{\partial^2 v}{\partial z^2}\right|_{z=0} = -\frac{E}{\cos\phi} \left.\frac{\partial^3 \Psi}{\partial z^3}\right|_{z=0} = \sqrt{\frac{E}{2|\mu|}} \left(\frac{\partial T_s}{\partial \phi}\right) \times \frac{(a + b) + e^{-\lambda}[(c + d)\sin\lambda - (c - d)\cos\lambda]}{e^{4\lambda} - 2e^{2\lambda}\sin 2\lambda - 1}, \quad (39)$$

where

$$a = -e^{4\lambda} + e^{\lambda}\cos(\lambda) + e^{3\lambda}\cos(\lambda) - e^{2\lambda}\cos(2\lambda) + e^{2\lambda}\sin(2\lambda)$$

$$b = -e^{4\lambda} + 2e^{3\lambda}\cos(\lambda) - e^{2\lambda}\cos(2\lambda) + e^{\lambda}\sin(\lambda) + e^{3\lambda}\sin(\lambda) - e^{2\lambda}\sin(2\lambda)$$

$$c = -e^{2\lambda} - e^{4\lambda} + e^{\lambda}\cos(\lambda) + e^{3\lambda}\cos(\lambda) - e^{\lambda}\sin(\lambda) + e^{3\lambda}\sin(\lambda) + e^{2\lambda}\sin(2\lambda)$$

$$d = e^{2\lambda} - e^{\lambda}\cos(\lambda) - e^{3\lambda}\cos(\lambda) + e^{2\lambda}\cos(2\lambda) - e^{\lambda}\sin(\lambda) + e^{3\lambda}\sin(\lambda)$$

and $\lambda \equiv \sqrt{|\mu|/(2E)}$, $T_s(\mu)$ is the equilibrium surface temperature distribution [i.e., $T_s(\mu) = T_E(\mu, 0)$].

For $\mu \neq 0$ and E small, we have $\lambda \to \infty$. Equation (39) becomes[4]

$$\frac{\partial \Phi_0}{\partial \phi} \approx -\sqrt{\frac{2E}{|\mu|}} \left(\frac{\partial T_s}{\partial \phi}\right), \quad \mu \geqslant \mu_b^+ \text{ or } \mu \leqslant \mu_b^-, \quad \text{for } E \ll 1. \quad (40)$$

Equation (40) can be used together with (36) to determine the extent of the Hadley circulation for various small values of E. Note that as $E \to 0$, Φ_0 is a constant for $\mu \neq 0$.

f. Upwelling and heating at the ITCZ

The vertical velocity in the circulation region is given by (27). Integrating the vertical velocity from south pole to north pole, we have

$$\mathrm{Ro}\delta_s \int_{-1}^{1} w d\mu = q(z) + \int_{-1}^{1} \frac{T_E - T}{\tau_0} d\mu. \quad (41)$$

Since the temperature T differs from T_E in the circulation region only,

$$\int_{-1}^{1} (T_E - T)d\mu = \int_{\mu_*^-(z)}^{\mu_*^+(z)} (T_E - T_M)d\mu, \quad (42)$$

where $\mu_*^{\pm}(z)$ are the northern and southern boundaries of the circulation region at height z. Thus, from (29), we have for the strength of the concentrated heating:

$$q(z) = -\frac{1}{\tau_0} \int_{\mu_*^-(z)}^{\mu_*^+(z)} (T_E - T_M)d\mu. \quad (43)$$

[4] The continuity of $\partial\Phi/\partial\phi$ near the edge of the Hadley region is invoked. Equation (40) is thus assumed to hold at the edge as well as outside.

5. Some examples

a. Symmetric equilibrium temperature

For an equatorially symmetric surface temperature profile, we assume, in this explicit example, that the vertical profile of the equilibrium temperature is a linear function of the height starting from a prescribed surface temperature $T_s(\mu)$ with a lapse rate Γ ($\geq\Gamma_m$) at each latitude (except at μ_1):

$$T_E(\mu, z) = T_s(\mu) - \Gamma z, \quad \mu \neq \mu_1. \tag{44}$$

In the nondimensional form, we have

$$T_E = \frac{R_H}{\mathrm{Ro}}[T_s(\mu) - \Delta_V z] \quad \mu \neq \mu_1. \tag{45}$$

At the ITCZ, μ_1, the convective–radiative equilibrium temperature, is given by (14):

$$T_E = T_M(z) \equiv \frac{R_H}{\mathrm{Ro}}(T_{M0} - \Delta_M z), \tag{46}$$

where surface temperature T_s is given by an equatorially symmetric distribution

$$T_s(\mu) = T_{00} - \Delta_H \mu^{2n}. \tag{47}$$

From (43), we know

$$q(0) = \frac{1}{\tau_0}\int_{-\mu_1}^{\mu_1} [T_{M0} - (T_{00} - \Delta_H \mu^{2n})]\, d\mu.$$

As for the ITCZ, we require $q(z) \geq 0$, otherwise there will not be moisture convergence into the convection region. Considering $T_s(\mu_1) = T_{00} - \Delta_H \mu_1^{2n}$ and $q(0) \geq 0$, we need

$$T_{M0} - T_s(\mu_1) > \frac{2n}{2n+1}\Delta_H \mu_1^{2n}. \tag{48}$$

Thus, if T_{M0} is given by $T_s(\mu_1)$, to have an ITCZ located at μ_1 for a symmetric T_E given by (44) the only possible location of the ITCZ is the latitude with warmest surface temperature.[5] This result is consistent with studies of the statistical relationship between sea surface temperature and cumulus activity, which suggest that high SST is a necessary condition for the intensive cumulus activity (Graham and Barnet 1987).

From (36), we know the boundary of the circulation region is determined by

$$\frac{R}{\mathrm{Ro}}\left[\mu^{2n} z_* + (\delta - \delta_m)\frac{z_*^2}{2}\right] = \frac{\mu^4}{8\,\mathrm{Ro}(1-\mu^2)} - [\Phi_0(\mu_1) - \Phi_0(\mu)], \tag{49}$$

where δ and δ_m are nondimensional lapse rates corresponding to Γ and Γ_m, respectively. For mathematical simplicity, we take $\Gamma = \Gamma_m$ and $n = 1$ as an example. (The difference between Γ_m and Γ will result in a slightly wider extent of circulation region and a slight enhancement of meridional circulation strength.) For simplicity, in the following calculation we choose $U = gH\Delta_H/(2\Omega a)$, and consequently $\mathrm{Ro} = R$. In the nearly inviscid limit, $E \to 0^+$, $\Phi_0(\mu)$ is a constant, and so (49) gives

$$z_* = \frac{\mu^2}{8R(1-\mu^2)}; \quad \text{or} \quad \mu_*^{\pm} = \pm\sqrt{\frac{8Rz}{1+8Rz}}. \tag{50}$$

The Hadley circulation in this symmetric case has zero width at the bottom in the inviscid limit. Setting $z = 1$ in (49) gives the extent of the Hadley circulation at the top boundary[6]:

$$\mu_t^{\pm} = \pm\sqrt{\frac{8R}{1+8R}} \tag{52}$$

This formula is similar to that in Satoh (1994) with $C \to \infty$.[7] From (44), we have the strength of the concentrated heating in the ITCZ

$$q(z) = \frac{2}{3\tau_0}\mu_*^3(z) = \frac{2}{3\tau_0}\left(\frac{8Rz}{1+8Rz}\right)^{3/2}. \tag{53}$$

The vertical velocity and meridional velocity are

$$w = \frac{\Delta_H}{R\Delta_s} q(z)\delta(\mu) - \frac{\Delta_H}{R\Delta_s\tau_0}\mu^2, \tag{54}$$

$$v\cos\phi = \frac{\Delta_H}{2R\Delta_s} q'(z)\,\mathrm{sgn}(\mu), \tag{55}$$

where $\Delta_s \equiv (\Gamma_d - \Gamma_m)H/T_0$ and the streamfunction is

$$\Psi = \frac{\Delta_H}{3R\Delta_s\tau_0}\begin{cases}[\mu_*(z)^3 - \mu^3] & \text{if} \quad \mu > 0\\ -[\mu_*(z)^3 + \mu^3] & \text{if} \quad \mu < 0.\end{cases} \tag{56}$$

[5] More precisely, the ITCZ should be located at the latitude with highest virtual surface air temperature, which may not necessarily be the latitude with highest surface temperature due to the high content of moisture in the ITCZ.

[6] For $n = 2$ and in the "inviscid limit," it gives $z_* = 1/[8R(1-\mu^2)]$, and the extent of the Hadley circulation at the top is given by

$$\mu_t^{\pm} = \pm\sqrt{\frac{1-8R}{8R}}. \tag{51}$$

It is found that there does not exist an angular momentum conserving circulation region unless $R > 1/8$. The solution for $R < 1/8$ was given in Fang and Tung (1994). For $R > 1/8$ the circulation region is detached from the lower surface. It starts from $z_*(0) = 1/(8R)$ rather than from the lower boundary.

[7] In Satoh (1994), if viscosity ν is fixed and the difference step in z direction, $dz \to 0$, the friction coefficient C approaches infinity.

The streamlines (outside viscous boundary layers) and the circulation region are shown in Fig. 2a. Note that there is a thin viscous boundary layer near the top (not shown) where the poleward meridional flow occurs. The dimensional streamfunction Ψ_d can be written as

$$\Psi_d = \rho_0 aHU\Psi = \rho_0 a^2 \times \frac{\Delta_H T_0}{3(\Gamma_d - \Gamma_m)\tau_0} \begin{cases} [\mu_*(z)^3 - \mu^3] & \text{if } \mu > 0 \\ -[\mu_*(z)^3 + \mu^3] & \text{if } \mu < 0. \end{cases}$$

The value of the parameters used are $R = 0.03$ and $\Delta_H = 1/6$, $\Gamma = 6$ deg km^{-1}, $\Gamma_d = 9.8$ deg km^{-1}, $H = 15$ km, $T_0 = 300$ deg, and $\tau = 20$ days. The total mass flux as a dimensional variable is 1.12×10^{10} kg s^{-1} in each hemisphere, which is more than twice as strong as the symmetric case obtained by Lindzen and Hou (1988) (4.6×10^9 kg s^{-1}). It is found that the strength of the circulation is proportional to horizontal temperature gradient ($\Delta_H T_0$) and is inversely proportional to the relaxation time and the static stability for a fixed thermal Rossby number R. Inside the Hadley circulation region, the temperature is given by T_M in (24) and the zonal wind is given by angular momentum conserving wind u in (19). Outside the Hadley circulation region, the temperature is given by the equilibrium temperature T_E (46) and the zonal wind is given by the equilibrium zonal wind u_E in (32). Figure 2b shows the temperature distribution (solid lines) and the equilibrium temperature (dashed lines). The zonal wind is shown in Fig. 2c. Note the discontinuity of the temperature and zonal velocity across the lateral edge of the Hadley cell. Such a solution is, strictly speaking, valid only in the limit of $E \to 0$. For E small but nonzero, there will be a viscous boundary layer near the interface and there will be a viscous correction to the leading-order asymptotic solution.

1) Viscous corrections: Extent of the Hadley cell

The solution given in (50) for the location of the edge of the Hadley cell is valid in the limit $E \to 0$. For small but nonzero values of E it can be shown that the viscous correction to (50) is minor near the top, but can be significant near the bottom, where the limiting width of the Hadley cell in (50) is zero. Substituting (38) and (39) into (49), with $T_s(\mu)$ given by (47), we find the modified location for various Es. This is depicted in Fig. 3 for various values of E. As expected, the width of the Hadley cell near the surface is sensitive to E since it is very sensitive to the small value of $\Phi_0(0) - \Phi_0(\phi_*)$. [$\mu_b \sim (\Phi_0(0) - \Phi_0(\mu_b))^{1/4} \sim E^{1/8}$ from (49).] In general, the width is nonzero. This fact is physically significant because it is the convergence in the lower viscous boundary layer that is supplying the necessary moisture for convection in the ITCZ.

2) Viscous corrections: Boundary layer near the edge of the Hadley cell

When E is small but nonzero, there is in general a viscous correction to the leading order solution whenever there is a sharp gradient. Because, as seen in Fig. 2a, there is a discontinuity in temperature across the lateral edge of the circulation region, there exists a layer near the edge where $E/\sigma\nabla^2 T$ is not negligible even for small E. An "inner friction layer" (actually "thermal" in the present case) is present near $z = z_*(\mu)$, and a singular perturbation analysis needs to be performed here.

As in section 3a, we let $(\hat{v}, \hat{w}) = (v, w)/\tau_0$. Equation (15) is written as

$$\mathrm{Ro}\left[\hat{v}\frac{\partial T}{\partial \phi} + \hat{w}\left(\frac{\partial T}{\partial z} + \delta_d\right)\right] = \frac{E\tau_0}{\sigma}\nabla^2 T + (T_E - T). \quad (57)$$

The thermal diffusion term, the first term on the right-hand side of (57), now needs to be retained even for small $E\tau_0$, because of the high gradients of T across the boundary layer. Since the interface $\mu = \mu_*(z)$ is a streamline, we expect the most rapid varying direction to be perpendicular to the streamline. It is now convenient to introduce the streamline coordinates, following Batchlor (1956).

Let $\hat{\Psi}$ be the streamfunction defined by

$$\hat{v}\cos\phi = -\frac{\partial \hat{\Psi}}{\partial z}$$

and

$$\hat{w} = \frac{\partial \hat{\Psi}}{\partial \phi}.$$

Let $\hat{\eta}$ = const lines be everywhere perpendicular to the streamlines $\hat{\Psi}$ = const, such that $(\hat{\Psi}, \hat{\eta})$ now form a two-dimensional orthogonal coordinate system.

Since $|\partial T/\partial \hat{\Psi}| \gg |\partial T/\partial \hat{\eta}|$ in the inner boundary layer near the edge of the circulation region, we have asymptotically,

$$\nabla^2 T = \nabla\cdot\nabla T \approx \nabla\hat{\Psi}\frac{\partial}{\partial \hat{\Psi}}\nabla\hat{\Psi}\frac{\partial T}{\partial \hat{\Psi}} \approx h^2\frac{\partial T}{\partial \hat{\Psi}^2}, \quad (58)$$

where $h^2 \equiv |\nabla\hat{\Psi}|^2 = (\hat{v}^2\cos^2\phi + (H/a)^2\hat{w}^2)$.

Upon introduction of the stretched boundary layer coordinate

$$(\xi, \eta) \equiv (\hat{\Psi}/\sqrt{E\tau_0/\sigma}, \hat{\eta}),$$

Eq. (57) now becomes

$$\mathrm{Ro}\left(|\nabla\eta|\frac{\partial T}{\partial \eta} + \delta_d\hat{w}\right) = h^2\frac{\partial^2 T}{\partial \xi^2} + (T_E - T). \quad (59)$$

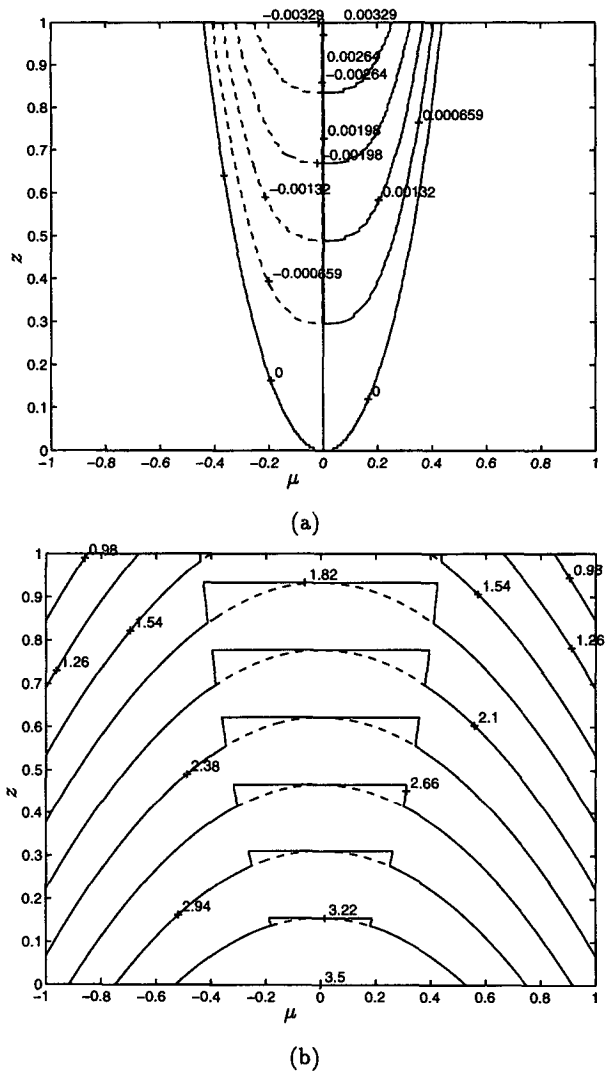

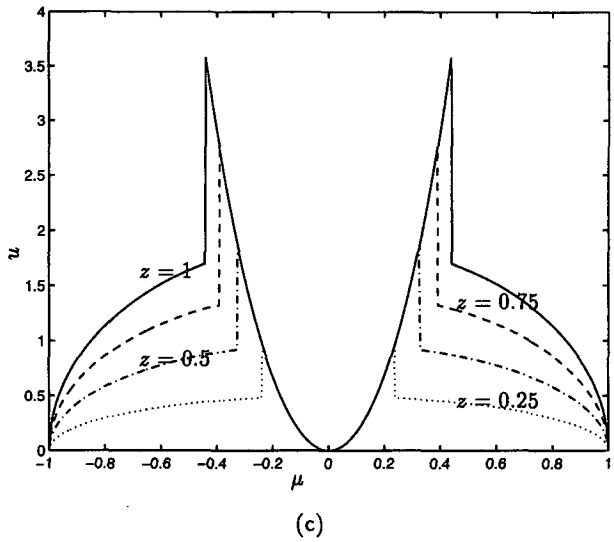

FIG. 2. Analytic inviscid solution for an equatorially symmetric surface temperature: (a) Stream function Ψ; (b) temperature T (solid lines) and equilibrium temperature T_E (dashed lines) distribution; and (c) zonal wind u at various altitudes.

The left-hand side is small for Ro $\ll 1$ (which is valid for the terrestrial atmosphere), and so

$$h^2 \frac{\partial^2 T'}{\partial \xi^2} - T' = 0, \tag{60}$$

where T' is the viscous correction to the leading-order solution. In (60), h^2 is taken to be independent of ξ and is given by leading-order solution obtained earlier in the limit $E \to 0$. The solution to (60) on different side is

$$T' = \begin{cases} 0.5(T_M - T_E)\exp(-\xi/h) & \text{for} \quad \xi > 0 \\ 0.5(T_M - T_E)\exp(\xi/h) & \text{for} \quad \xi < 0, \end{cases} \tag{61}$$

which satisfies the asymptotic matching condition:

$$T \to T_E, \quad \xi \to \infty; \quad T \to T_M, \quad \xi \to -\infty;$$
$$\text{and} \quad T = 0.5(T_M - T_E), \quad \xi = 0.$$

The use of curvilinear coordinates turns out to be cumbersome for expressing the result of (61) in terms of physical coordinates. This process can be simplified by replacing the curvilinear coordinate (ξ, η) by a local linear coordinate (ξ', η') defined by

$$\eta' = \frac{1}{\sqrt{1+k^2}}[(\mu - \mu_0) + k(z - z_0)];$$
$$\xi' = \frac{1}{\sqrt{1+k^2}}[k(\mu - \mu_0) - (z - z_0)], \tag{62}$$

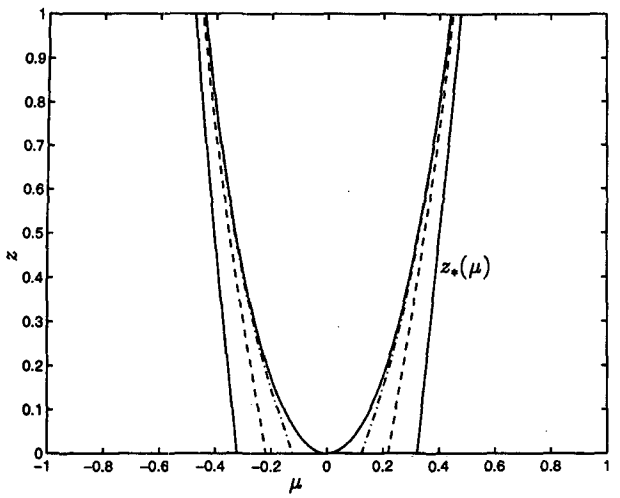

FIG. 3. The viscous effect on the extent of the circulation. The extent of the circulation is for $E = 0$ (solid), $E = 2 \times 10^{-4}$ (dash-dotted), $E = 3 \times 10^{-3}$ (dashed), and $E = 2.5 \times 10^{-2}$ (outer solid).

where (μ_0, z_0) is the edge of the Hadley cell and $k \equiv (dz_*(\mu)/d\mu)|_{\mu_0}$ is the local slope of the edge. The new coordinate is identical to the old curvilinear coordinate at (μ_0, z_0). Thus, except for an exponentially small error, (60) can be approximated by

$$h'^2 \frac{\partial^2 T'}{\partial \xi'^2} - T' = 0, \qquad (63)$$

where $h'^2 = ((\partial\xi'/\partial z)^2 + (H/a)^2(\partial\xi'/\partial\mu)^2)|_{(\mu_0,z_0)}$. The new solution is the same as (61), except with h' replacing h and ξ' replacing ξ. It is plotted in Fig. 4a for various values of $\sqrt{E\tau_0/\sigma}$. It is seen that the jump in T in the limiting solution $E \to 0$ (Fig. 2a) is replaced by a smooth transition from T_M on one side to the equilibrium T_E on the other side of the boundary layer. The degree of smoothness increases with $\sqrt{E\tau_0/\sigma}$. This analytic solution will later be verified by the numerical solution in section 6.

Once the temperature is obtained with viscous correction, the corresponding zonal wind can be obtained easily using the thermal wind relationship (22). One can easily show, using the viscous meridional momentum equation (11), that the thermal wind relationship holds even inside the inner boundary layer. This is because the leading-order solution for v is continuous, and so the viscous term $E\nabla^2 v$ is of order E. The nonlinear advection of the meridional velocity is $O(1/\tau_0^2)$ and so is also small. The zonal winds for various values of E are plotted in Fig. 4b.[8] The asymptotic solution will also be verified numerically in section 6.

[8] Some interpolation across the equator is needed for the viscous solutions.

3) LOCATION OF THE ITCZ

Any $\mu_1 \neq 0$ in the case of symmetric surface temperature will lead to a negative $q(z)$ from (47). It implies that for a symmetric equilibrium temperature distribution, the ITCZ should be located at the latitude of warmest sea surface temperature. However, when the viscous effect is taken into account, it could shift slightly off the equator (we will discuss it in the next section).

However, for a surface temperature without a distinctive maximum at the equator but with a broad peak near the equator, as used by Numaguti (1993) for describing the distribution of SST in middle and western Pacific:

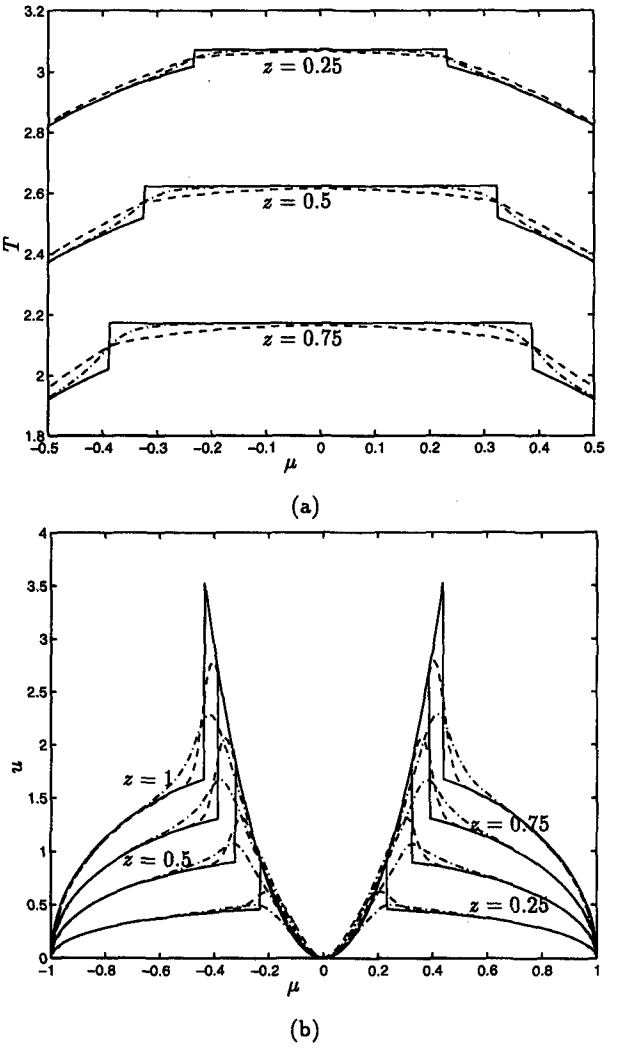

FIG. 4. Viscous correction to "inviscid limit" at various altitudes, with solid lines for "inviscid limit"; dashed lines for $\epsilon \equiv (E\tau_0/\sigma)^{1/2} = 0.16$; dash-dotted lines for $\epsilon = 0.04$: (a) Temperature T; (b) Zonal wind u.

$$T_S(\mu) = \begin{cases} \dfrac{R_H}{\mathrm{Ro}}(T_{00} - \Delta_H \mu_p^2) & \text{if} \quad |\mu| < \mu_p \\ \dfrac{R_H}{\mathrm{Ro}}(T_{00} - \Delta_H \mu^2) & \text{elsewhere,} \end{cases} \tag{64}$$

where μ_p is the width of the broad peak region. We find that the ITCZ still occurs over the warmest surface temperature, but now there is no preferred location for the ITCZ within this broad peak region. There is a possibility that two ITCZs can coexist at both sides of the equator, at $\pm\mu_1$, and a pair of weak reversed circulation cells exist between $-\mu_1$ and μ_1. Figure 5 shows the contour of the meridional circulation for $\mu_1 = \mu_p = 0.1$, $\Gamma = 7$ deg km^{-1}, $\Gamma_m = 6$ deg km^{-1}, and other physical parameters the same as those used in Fig. 2.

b. Asymmetric equilibrium temperature

In the eastern Pacific region, the SST has a local minimum at the equator due to strong oceanic upwelling. The maximum of SST is usually located in the Northern Hemisphere. As an example, when the surface temperature is asymmetric about the equator, we use [same as in Lindzen and Hou (1988)], for $\mu \neq \mu_0$,

$$T_E = \frac{R_H}{\mathrm{Ro}}[T_{00} - \Delta_H(\mu - \mu_0)^2 - \Delta_V z], \tag{65}$$

and

$$T = T_M(z) = \frac{R_H}{\mathrm{Ro}}(T_{M0} - \Delta_M z) \tag{66}$$

in the circulation region. For simplicity, we take $\Delta_V = \Delta_M$. We now proceed to find the boundary of the Hadley region. *Suppose* at latitude μ_*, the top boundary is in the circulation region while the bottom boundary is not—that is, $\mu_b^+ < \mu_* < \mu_t^+$ or $\mu_t^- < \mu_* < \mu_b^-$ (the situation is depicted in Fig. 1). From (36) and (39), we have

$$[(\mu_* - \mu_0)^2 - (\mu_1 - \mu_0)^2]z_* = \Phi_0(\mu_*) - \Phi_0(\mu_1) + \frac{(\mu_*^2 - \mu_1^2)^2}{8R(1 - \mu_*^2)} \tag{67}$$

and $\Phi_0(\mu_*) - \Phi_0(\mu_1) = O(\sqrt{E})$. Here, we still choose $U = gH\Delta_H/(2\Omega a)$ and $\mathrm{Ro} = R$. In the latitudes where there is circulation above the bottom boundary—that is, $\mu_b^- < \mu_* < \mu_b^+$—(36) gives

$$z_* = 0;$$

and

$$\Phi_0(\mu) = \Phi_0(\mu_1) - \frac{(\mu^2 - \mu_1^2)^2}{8\,\mathrm{Ro}(1 - \mu^2)}. \tag{68}$$

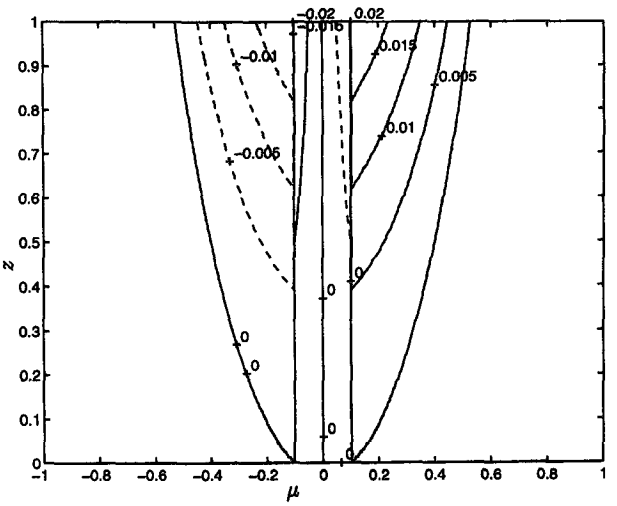

FIG. 5. The stream lines in the "inviscid core" for a symmetric surface temperature with a broad maximum from −0.1 to 0.1.

Similar to the discussion for the symmetric temperature, if we set $\Phi_0(\mu_*) - \Phi_0(\mu_1) = 0$ in the nearly inviscid limit, the extent of circulation at the bottom boundary $z_* = 0$ is given by $\mu_b^\pm = \pm\mu_1$. For $|\mu| > \mu_1$, (66) gives[9]:

$$z_* = \frac{(\mu + \mu_1)^2(\mu - \mu_1)}{8R(1 - \mu^2)(\mu + \mu_1 - 2\mu_0)}. \tag{69}$$

The extent of the circulation at the top boundary is obtained by setting $z_* = 1$ in (69):

$$(\mu_t + \mu_1)^2(\mu_t - \mu_1) - 8R(1 - \mu_t^2)(\mu_t + \mu_1 - 2\mu_0) = 0. \tag{70}$$

As $\mu_1 \to \mu_0$, the top extent has a simple formula

$$\mu_t^\pm = \frac{-\mu_0 \pm \sqrt{8R(1 + 8R) - 8R\mu_0^2}}{1 + 8R}. \tag{71}$$

This is the same as obtained previously by Satoh (1994), who, however, did not obtain the location of the boundary at other heights.

From (43), we also can obtain the strength of the net heating in the ITCZ:

$$q(z) = \frac{1}{3\tau_0}[(\mu_*^+ - \mu_0)^3 - (\mu_*^- - \mu_0)^3 - 3(\mu_1 - \mu_0)^2(\mu_*^+ - \mu_*^-)], \tag{72}$$

[9] The case of $\mu_1 = \mu_0$ needs to be considered as the limit of the case of $\mu_1 = \mu_0 + \epsilon$ as $\epsilon \to 0^+$.

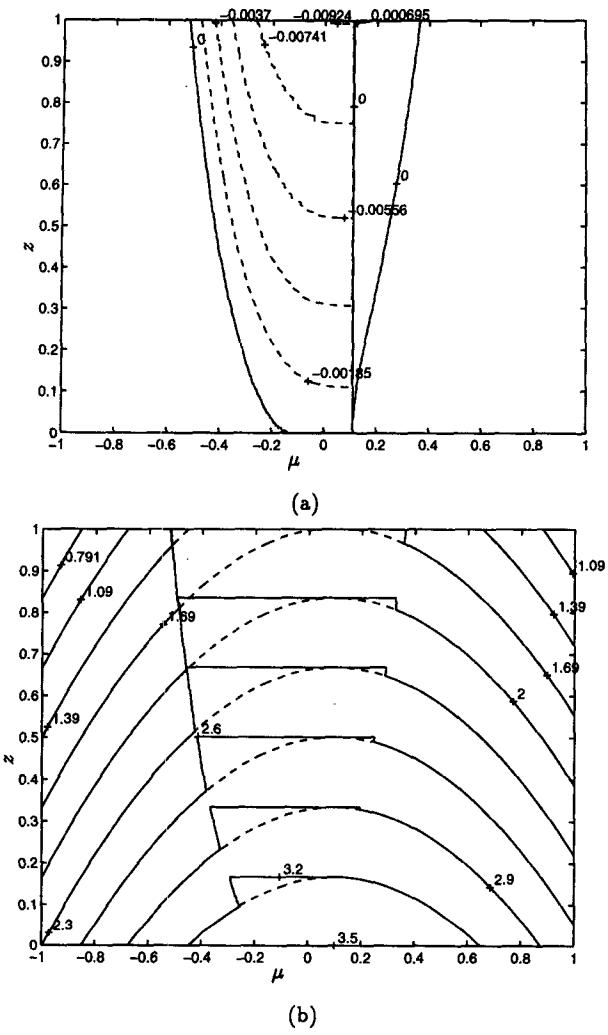

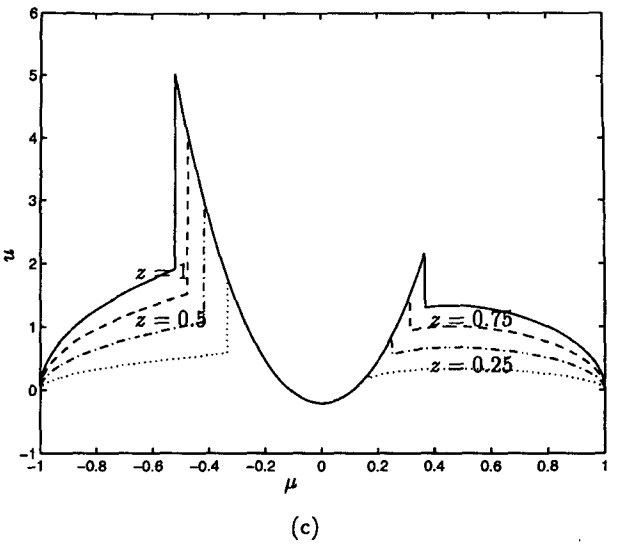

FIG. 6. Analytic inviscid solution for an equatorial asymmetric surface temperature ($\mu_0 = 0.1$, $\mu_1 = 0.11$): (a) Stream function Ψ; (b) temperature T (solid lines) and equilibrium temperature T_E (dashed lines) distribution; and (c) zonal wind u at various altitudes.

where $\mu_*^{\pm}(z)$ are the locations of the edge of the circulation cell at altitude z in summer and winter hemisphere, and "plus" or "minus" signs corresponds to $\mu > \mu_1$ and $\mu < \mu_1$, respectively. The location of the ITCZ is constrained by the requirement: $q(z) \geq 0$. In particular, it is required that

$$q(0) = \frac{1}{3\tau_0}[(\mu_1 - \mu_0)^3 - (-\mu_1 - \mu_0)^3 - 6\mu_1(\mu_1 - \mu_0)^2] \geq 0. \quad (73)$$

Assuming the mass is conserved at each circulation cell, we have the streamfunction:

$$\Psi^{\pm} = k[(\mu_*^{\pm} - \mu_0)^3 - (\mu - \mu_0)^3 - 3(\mu_1 - \mu_0)^2(\mu_*^{\pm} - \mu)], \quad (74)$$

where $k \equiv \Delta_H/(3R\Delta_S\tau_0)$. The streamlines and the circulation region are shown in Fig. 6a for $\mu_0 = 0.1$, $\mu_1 = 0.11$. Other parameters are the same as in the case of symmetric surface temperature. The dimensional mass flux of the circulation in the winter cell (3.14×10^{10} kg s^{-1}) is stronger than the asymmetric case obtained in Lindzen and Hou (1988) for the same μ_0 (2.2×10^{10} kg s^{-1})[10] and is also stronger than that obtained in our symmetric case. Our value is very close to the observational data obtained by Oort (1983). [Multiplying 2π to our value leads to 19.73×10^{10} kg s^{-1}, compared to the observed values in solstices (19.7×10^{10} kg s^{-1} in DJF, 1963–1973, and 18.1×10^{10} kg s^{-1} in JJA, 1963–1973).] The distribution of the temperature and the zonal wind are shown in Figs. 6b and 6c, respectively. Viscous corrections are

[10] In Lindzen and Hou (1988), $\Delta_S = 1/8 = 0.125$, while ours is 0.19. If we use their value, it will lead to an even stronger mass flux.

not shown. These generally tend to smooth out only the discontinuities in the limiting solution.

6. Numerical calculation

Numerical calculations have been performed for both equatorially symmetric and asymmetric equilibrium temperatures. The model used is described by Eqs. (1)–(7), which is basically the same set of Boussinesq primitive equations as in Held and Hou (1980), except here the vertical temperature profile in the ITCZ is specified. The parameters used are the same as in the calculation of the analytic solutions in sections 5a and 5b. For simplicity, we take $\Gamma = \Gamma_m$ and $T_{M0} = T_s(\mu_1)$ in the calculations. The steady solution is obtained by integrating forward in time from a motionless and equilibrium temperature initial condition. At each time step, Eqs. (1)–(6) are solved for a uniform τ_0 in the whole domain and the temperature in the ITCZ is reset to its equilibrium value after each time. The $E \to 0^+$ case could not be done numerically since no steady solution can be reached via time stepping when E is below some value. The grid is a staggered grid with 50 points in the vertical and 180 points from the south pole to the north pole. The numerical scheme utilized is standard in all respects.

For the symmetric equilibrium temperature given by (44) and (47), a series of calculations have been completed for $E = 5 \times 10^{-5}$, 1×10^{-4}, 2×10^{-4}, 4×10^{-4}, and 8×10^{-4}. The geopotential at the lower surface, Φ_0, is shown in Fig. 7. It confirms the scaling mentioned earlier that the magnitude of $\Phi_0(\mu)$ is proportional to $\sqrt{E}$. The maximum values of $\Phi_0(\mu)$ versus $\sqrt{E}$ are plotted in Fig. 8. It is seen that it follows almost a perfect straight line, confirming the earlier result based on asymptotic scaling. In the following calculations, a "standard" Ekman number E is taken to be 4×10^{-4} ($\nu = 10\ \mathrm{m^2\ s^{-1}}$).

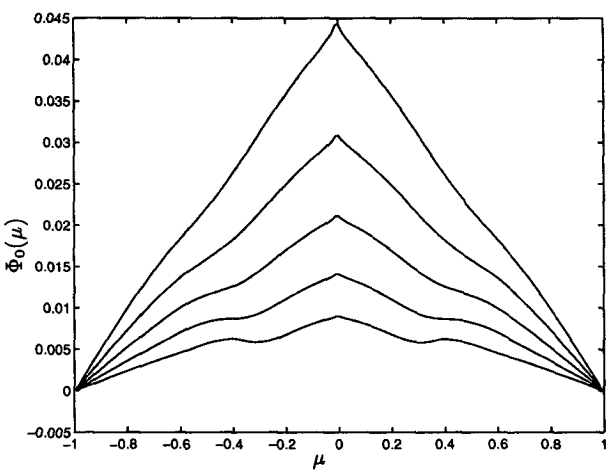

FIG. 7. The geopotential at the lower surface for $E = 5 \times 10^{-5}$, 1×10^{-4}, 2×10^{-4}, 4×10^{-4}, and 8×10^{-4} (the maximum value increases with E).

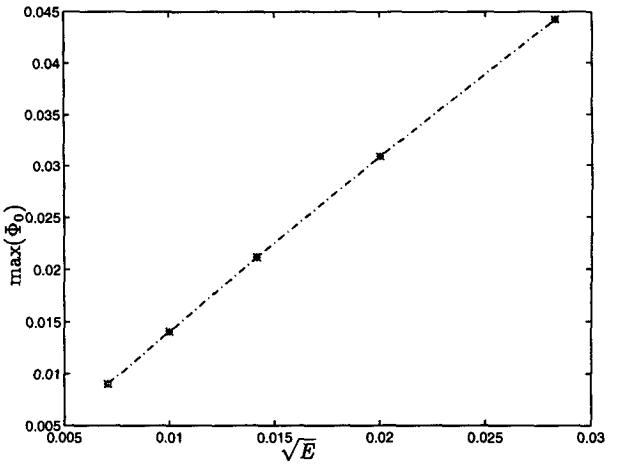

FIG. 8. The maximum values of $\Phi_0(\mu)$ vs $\sqrt{E}$.

Figure 9a shows the numerically obtained streamfunction solution for $E = 4 \times 10^{-4}$, while Fig. 9b shows the analytic streamfunction for small E. The analytic and numerical solutions are in good agreement with respect to the magnitude and the extent of the circulation in the "inviscid core." Compared with the analytic solution in the $E = 0$ case (Fig. 2), the strength of the circulation for $E = 4 \times 10^{-4}$ is about 20% less since the inviscid core extends up to $z \approx 0.85$ only. It is nevertheless still twice as strong as that obtained in Lindzen and Hou (1988). The latitudinal extent of the circulation near the bottom shrinks as E becomes small in the numerical solutions, as was founded earlier in our analytic solution. However, we could not obtain a numerical solution for an arbitrarily small E. The extent of the circulation at the lower surface is very sensitive to E. The numerical results also show that the poleward flow is confined in a narrow viscous boundary layer near the top.

Figure 10a shows the zonal wind at various altitudes, the numerical solution for $E = 4 \times 10^{-4}$ is shown in dotted lines and the analytic solution for $E = 4 \times 10^{-4}$ is shown in solid lines, while the $E = 0$ analytic solution is shown in dashed lines. The maximum jet speed of the numerical solution agrees very well with that of the analytic solution for small E. The agreement deteriorates slightly with respect to the position of the jet maximum closer to the surface. This is probably due to the fact that the asymptotic parameter $\epsilon \equiv \sqrt{E\tau_0}$ is not small enough for the analytic solution to be accurate, which was obtained under the assumption that the bottom viscous boundary layer does not overlap with the inner frictional layer. Figure 10b shows the distributions of temperature for $E = 4 \times 10^{-4}$. The numerical solution is shown in dotted lines. The analytic solution for

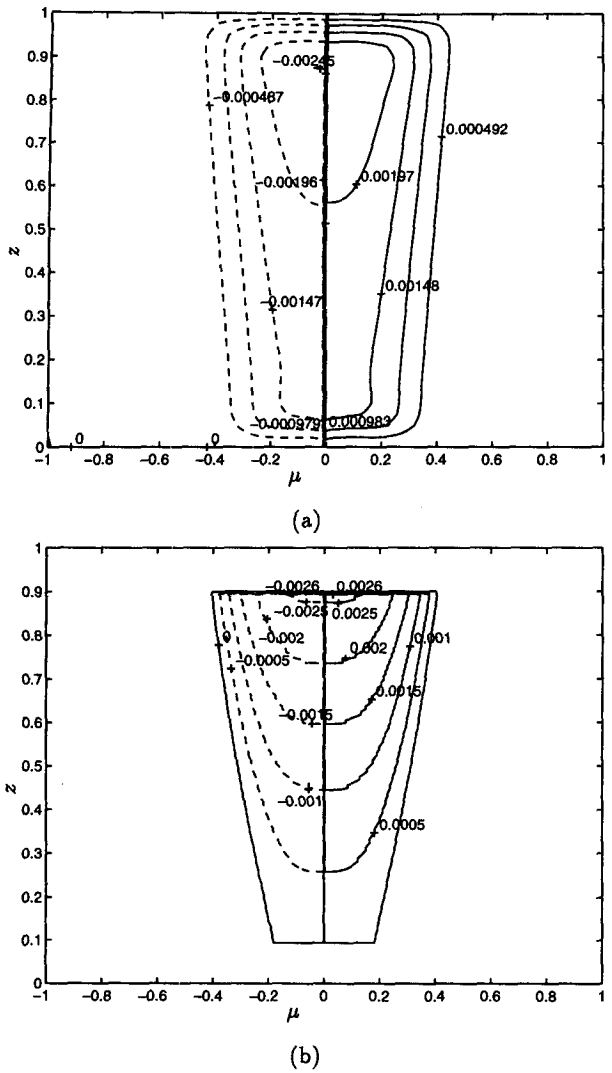

FIG. 9. The streamfunctions for $\mu_0 = 0$, $\mu_1 = 0$, and $E = 4 \times 10^4$: (a) Numerical result, and (b) analytic result.

$E = 4 \times 10^{-4}$ is shown in solid lines, while that for $E = 0$ is shown in dashed lines. In the circulation region, the latitudinal temperature gradient is approximately zero, as in the analytic solutions. The slight discrepancy near the midlatitude is mainly due to the use of local linear coordinate transform.

Figure 11 displays the numerical solution for an asymmetric equilibrium temperature given in section 5.2 ($\mu_0 = \mu_1 = 0.1$). Figure 11a shows the streamfunction. Due to an intensified circulation in the winter cell, the viscous effect becomes less effective and the strength of the circulation tends closer to the analytic solution for $E = 0$ (10% less). Figure 11b shows the zonal wind at the top and it is close to the $E = 0$ analytic solution in the winter cell. However, in the summer cell, the circulation cell becomes very weak ($1/12$ as strong as in the winter cell) and the viscosity has significant effect on the zonal wind. Figure 11c shows the distributions of the temperature for the numerical solution (solid lines) and the $E = 0$ analytic solution (dashed lines). It is also shown that the horizontal temperature profile is flat in most of winter cell and it presents a sharp gradient between the winter cell and the equilibrium region. In the summer cell, the temperature is very close to its equilibrium state.

The sensitivity test for the location of the ITCZ has been performed and the results are shown in the ap-

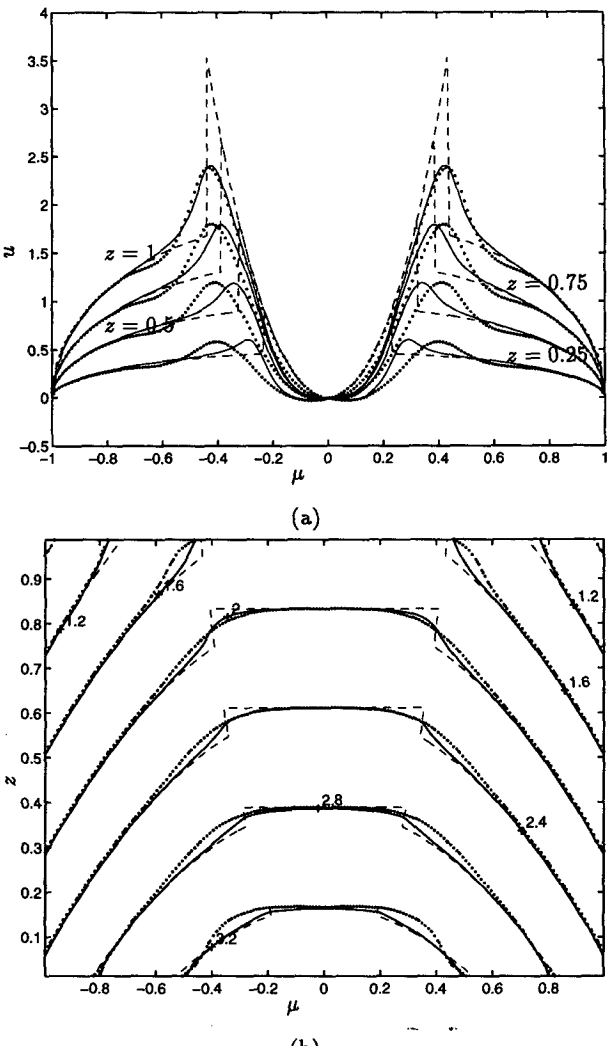

FIG. 10. Solution of zonal wind and the temperature for $\mu_0 = 0$, $\mu_1 = 0$, and $E = 4 \times 10^4$: (a) Zonal wind at various altitudes, where dotted lines are for the numerical result and solid lines for the analytic solution. The analytic solution for $E = 0$ is shown in dashed lines; (b) temperature distributions of the analytic solutions (solid lines), numerical solution (dotted lines), and analytic solution for $E = 0$ (dashed lines).

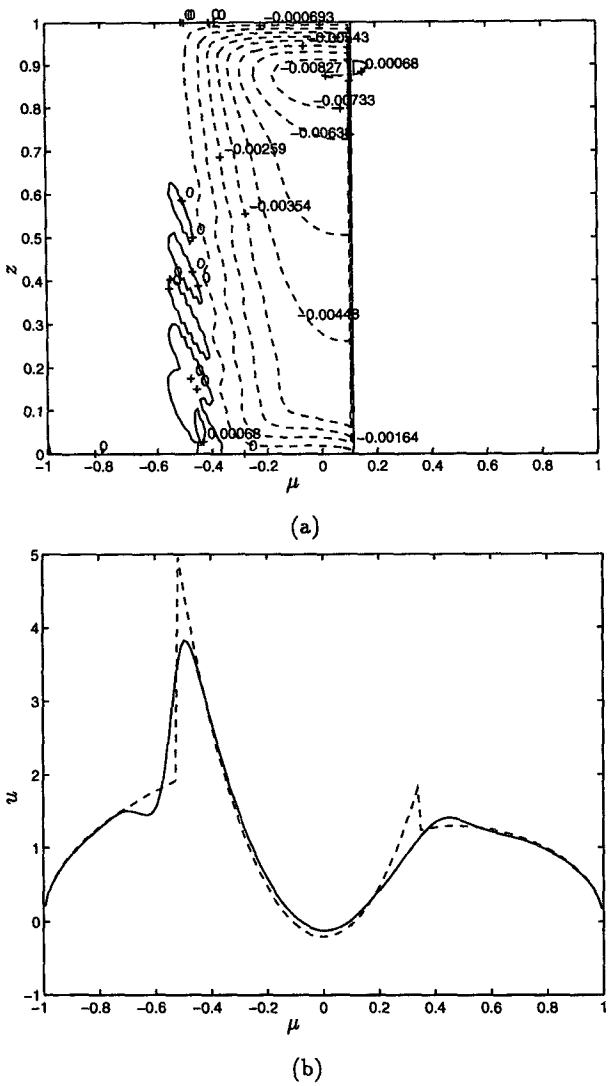

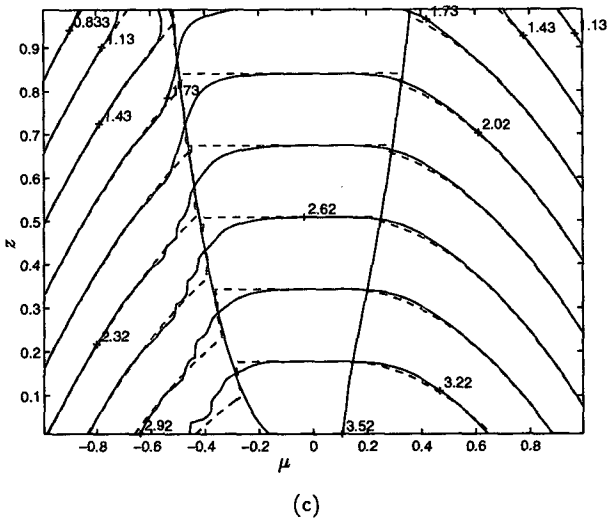

FIG. 11. Numerical solution for $\mu_0 = 0.1$, $\mu_1 = 0.1$, and $E = 10^{-4}$: (a) Contour of stream function; (b) zonal wind at the top, where solid line is for the numerical result and dashed line for the analytic solution in the "inviscid limit"; and (c) temperature distributions of the numerical solution (solid lines) and the "inviscid limit" (dashed lines).

pendix. Since the ITCZ is defined as the region where a strong mass convergence occurs, the net heating should be positive. This gives a constraint on the specification of μ_1 in our model. Based on our numerical solutions, it is found that although the location of the ITCZ does not necessarily coincide with the location of the warmest surface temperature, the two should not be too far separated.

In our calculation, since the resulting concentrated heating $q(z)$ has a maximum near the top, the streamfunction also has a single maximum near the top. This is supported by the observation (Oort 1983). This is different from that obtained by Hou and Lindzen (1992).

Our numerical calculation is repeated for a cyclostrophic model, that is, with the advection term in the meridional velocity equation ignored. The results show that there is no significant difference and confirm the conclusion obtained asymptotically that the cyclostrophic balance is a valid approximation in the adopted parameter regime ($\tau_0 \gg 1$).

7. Concluding remarks

The present work differs from previous papers on Hadley circulations (Held and Hou 1980; Lindzen and Hou 1988; Hou and Lindzen 1992) in that we assumed that in regions of intense moist convection (the ITCZ), the temperature profile locally adjusts to the moist adiabat on a timescale much faster than the Newtonian cooling relaxation time adopted by other authors. Therefore, the temperature there is known and not to be determined by the large-scale circulation. It is the net heating that needs to be determined as part of the solution. This approach is consistent with the concep-

tual model of Emanuel et al. (1994) and with the numerical result of Satoh (1994), which includes moist convection. Away from the region of intense convection, temperature adjusts radiatively on a slower timescale. The large-scale Hadley circulation is then responsible for determining the temperature distribution within the Hadley cell away from the ITCZ. The zonal absolute angular momentum in the inviscid core is found to be constant, which is an extension of the conclusion given by Batchelor (1956) for the case of steady 2D flow with closed streamlines. Thus, there is no horizontal gradient of the temperature inside the Hadley circulation cell at each height. The vertical temperature profile within the Hadley cell should follow the moist adiabat appropriate for the latitude of the ITCZ. This result is asymptotically valid in the limit of small viscosity ($E \to 0^+$) and large radiative relaxation time ($\tau_0 \gg 1$, dimensionally larger than a few hours). The strength of the Hadley circulation found this way is stronger than in the previous results and is now very close to the observed.

The studies in Emanuel et al. (1994), Yanai et al. (1973), and Satoh and Hayashi (1992) suggest that convection determines the vertical lapse rate approximately as the moist adiabat. Although the large-scale circulation does not alter this lapse rate in the Tropics, it does change the sea surface temperature and the subcloud-layer entropy in the context of a coupled ocean–atmosphere system. The strong large-scale circulation will reduce the magnitude of the surface temperature in the Tropics. This process is through a convective downdraft of low-entropy air and an increased surface heat flux to the ocean. As a simple decoupled model, this paper ignores this feedback of the large-scale circulation to the sea surface temperature. It also does not predict the location of the ITCZ. Nevertheless, our work suggests that, from mass balance consideration alone, the location of the ITCZ needs to be near the latitude of the warmest tropical sea surface temperature. Otherwise, there is not enough subsidence in the rest of the Hadley circulation region to support a rising branch in the ITCZ.

Another unrealistic assumption in this work is the imposition of a lid at the model troposphere. We have since repeated the calculations without lid, and can report that there is no significant change in the results unless the height of the ITCZ exceeds the tropopause, since there is no penetration of the Hadley circulation across the tropopause. (More precisely, $w = 0$ in the lower stratosphere if there is no horizontal gradient of T_E. In the presence of T_E gradient across the equator above the tropopause, there will be a circulation in the stratosphere. However, this is not an extension of the tropospheric Hadley circulation.)

Acknowledgments. We wish to thank Prof. Ed Sarachik and Dr. Hu Yang for their valuable discussions. The helpful comments by Dr. Isaac Held, Prof. Mankin Mak, and another reviewer are gratefully acknowledged. This research is supported by NASA Grant NAG-1-1404.

APPENDIX

Numerical Solution for $\mu_1 \neq \mu_0$

Numerical calculations for the cases when the ITCZ is not located at the latitude of the warmest surface temperature have also been performed. Figure A1 displays the solution for $\mu_0 = 0$, $\mu_1 = 0.1$. The contour of the streamfunction is shown in Fig. A1a. The strengths

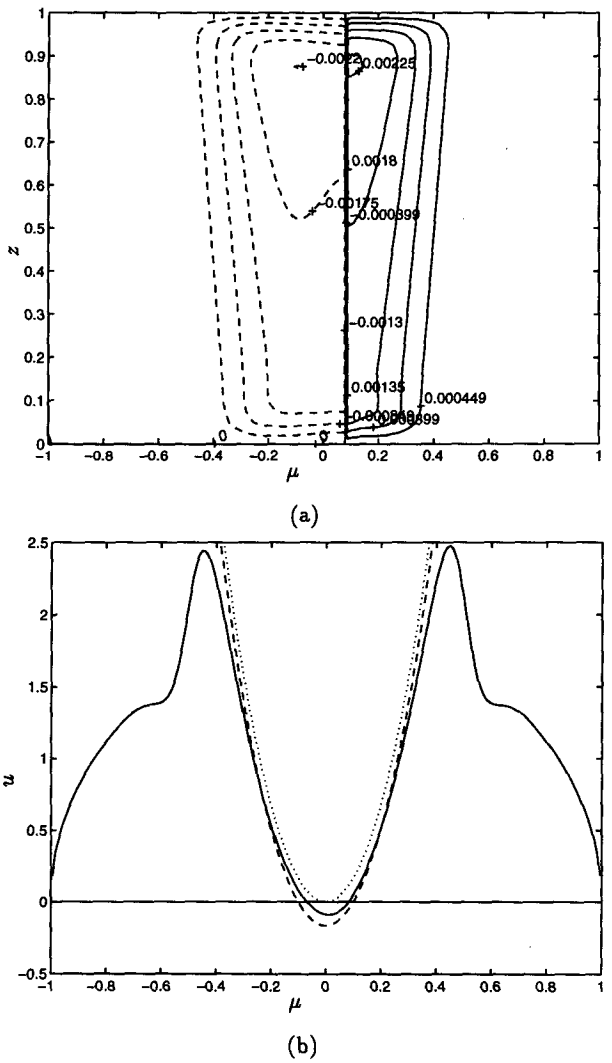

FIG. A1. Numerical solution for $\mu_0 = 0$, $\mu_1 = 0.1$: (a) Stream function and (b) zonal wind at the top, where solid line is for the numerical result, dotted line and dashed line are for the angular momentum conserving zonal wind originated from $\mu_1 = 0$, 0.1 respectively.

of two cells are equal but each is slightly weaker than its counterpart in Fig. 9a. The circulation region as a whole is still almost symmetric about the equator but it is separated at the ITCZ, and the winter cell has a larger size. According to the discussion in section 3a, the concentrated heat source $q(z)$ will be negative near the lower surface if $\mu_1 \neq \mu_0$ in the inviscid limit. But in the viscous case, $q(z)$ is still positive and, therefore, physically permissible due to the low-level return flow in the viscous boundary layer. Figure A1b shows the numerical solution for zonal velocities at the top in solid line. Also shown are the zonal winds calculated from (19), which is the expression of angular momentum conservation for a parcel rising from μ_s. The dotted

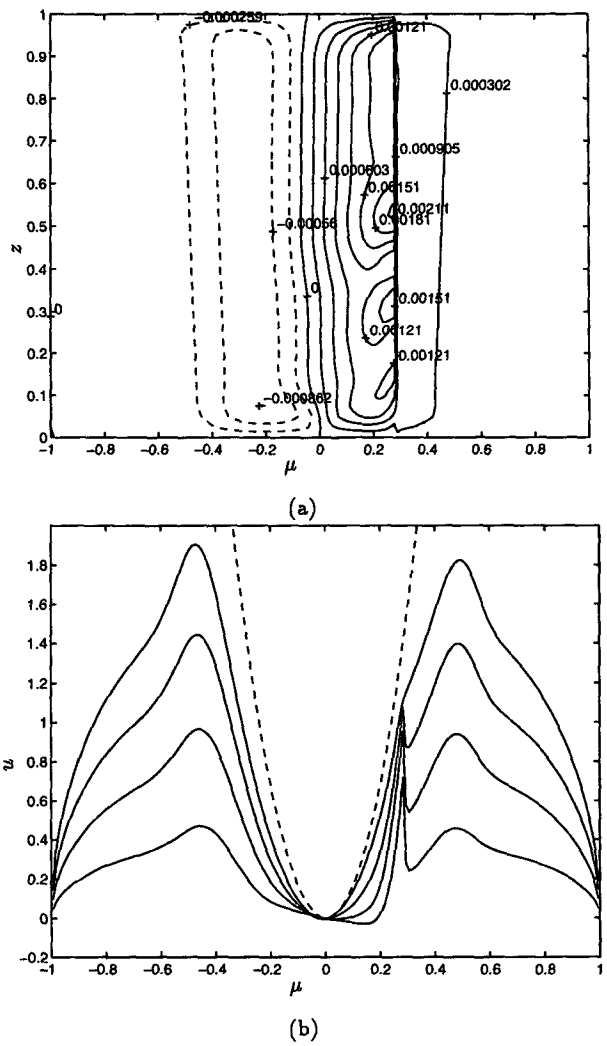

FIG. A2. Numerical solution for $\mu_0 = 0$, $\mu_1 = 0.3$: (a) Stream function; (b) Zonal wind at different altitudes ($z = 1$, 0.75, 0.5, 0.25 corresponding to the large value of the zonal wind to the small value respectively), and dotted line is for the angular momentum conserving zonal wind with $\mu_1 = 0$.

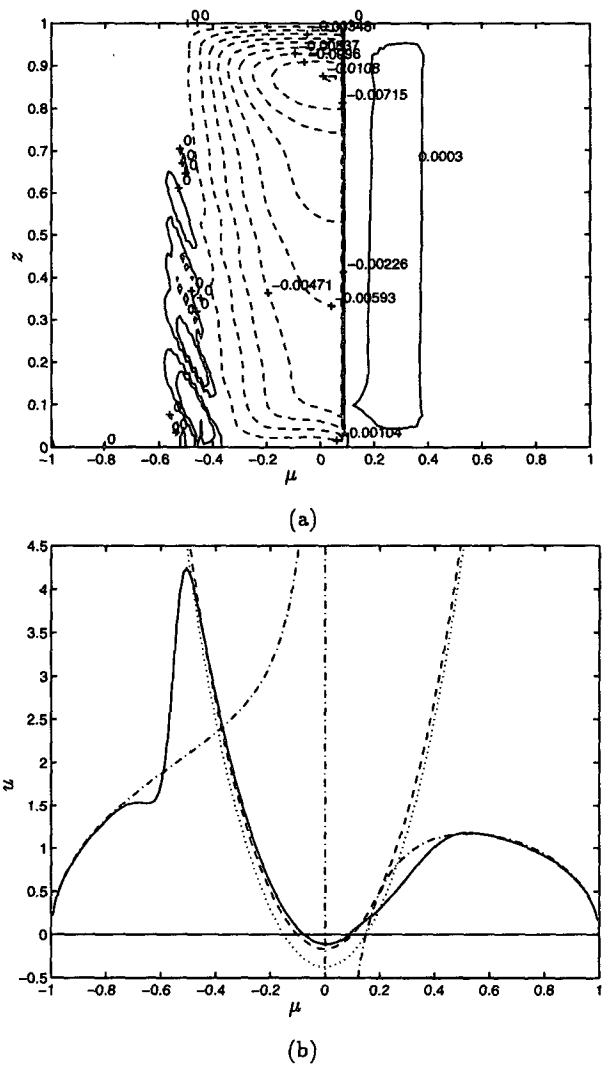

FIG. A3. Numerical solution for $\mu_0 = 0.15$, $\mu_1 = 0.1$: (a) Stream function and (b) zonal wind at the top, where solid line is for the numerical result, dashed line and dotted line are for the angular momentum conserving zonal wind for $\mu_1 = 0.1$, 0.15, respectively, and dash-dotted line is for the equilibrium zonal wind.

line is for $\mu_s = 0$ and the dashed line is for $\mu_s = 0.1$. It is seen that the numerically calculated zonal wind lies in between these two simple curves, and, therefore, we may conclude that the numerical solution for this case follows an angular momentum conserving path with the rising motion occurring in a wider region from 0 to 0.1. Because the circulation region is symmetric about the equator and the equilibrium temperature is symmetric, the zonal wind and the temperature are also symmetric about the equator.

When the ITCZ moves further poleward, the pattern of the circulation changes. Figure A2 displays the solution for $\mu_0 = 0$, $\mu_1 = 0.3$. The streamfunction is

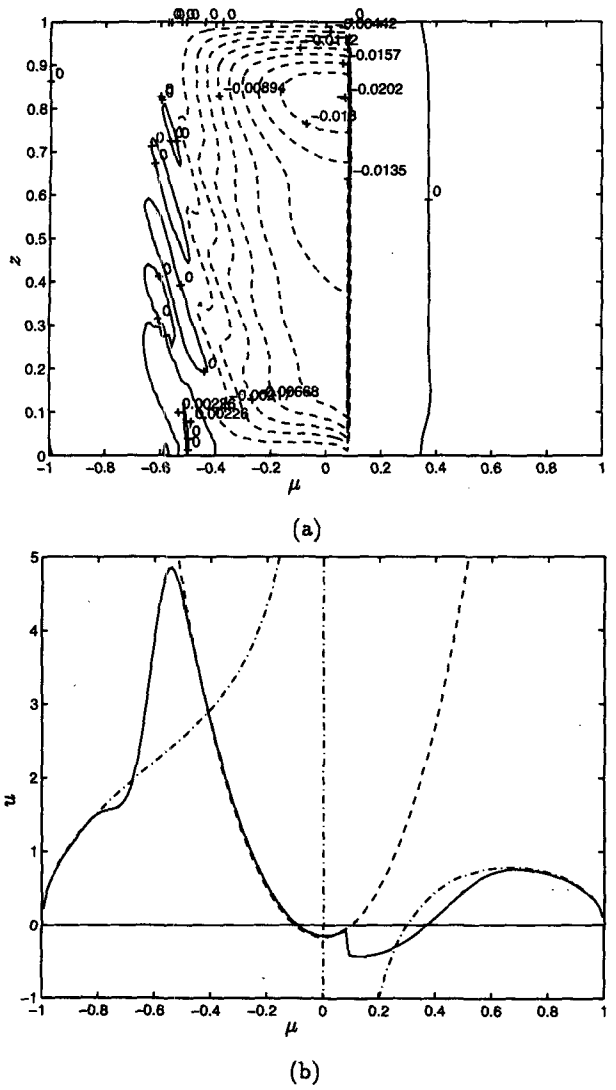

FIG. A4. Numerical solution for $\mu_0 = 0.3$, $\mu_1 = 0.1$: (a) Stream function; (b) zonal wind at the top, where solid line is for the numerical result, dashed line is for the angular momentum conserving zonal wind originated from $\mu_1 = 0.1$, and dash-dotted line is for the equilibrium zonal wind; (c) temperature distributions of the numerical result (solid lines) and the equilibrium state (dashed lines).

shown in Fig. A2a. It is found that the cell containing the ITCZ has a large size and a strong circulation, while the whole circulation domain is still symmetric about the equator. In this case, the concentrated heating $q_0(z)$ is negative and a sinking rather than rising motion occurs in the ITCZ. Thus, this case may not be physically relevant to the modeling of the latent heating in the ITCZ. Figure A2b shows the zonal wind at various altitudes ($z = 1, 0.75, 0.5, 0.25$), and the dashed line is the angular momentum conserving zonal wind when the rising motion occurs at the equator in (19). It is found that the zonal wind follows an angular momentum conserving path originated from μ_0 rather than μ_1, and the sinking motion at μ_1 carries the angular momentum downward. The temperature in this case is still symmetric about the equator.

For an asymmetric surface temperature, the circulation does not change if the ITCZ drifts slightly away from the warmest place poleward or equatorward. Figure A3 displays the solution for $\mu_0 = 0.15$, $\mu_1 = 0.1$. Figure A1a shows the streamfunction. A winter cell starts from μ_1 and it is slightly stronger than its counterpart in Fig. 11a since the difference between T_E and T is large in the winter cell. The summer cell is very weak and is viscosity dominated. Figure A3b shows the zonal wind at the top. It is found that the solution (solid line) follows an angular momentum conserving path where the rising motion occurs at the ITCZ [$\mu_s = 0.1$ in (19)] (dashed line) rather than a path where the rising motion occurs at the warmest place [$\mu_s = 0.15$ in (19)] (dotted line). The region of this angular momentum conserving zonal wind is from

$\mu_0 = 0.15$ to the whole winter cell. Poleward of $\mu_0 = 0.15$, the zonal wind is less than its equilibrium value (dash–dotted line). This region starts from μ_0 and extends poleward to the latitude where the equilibrium zonal wind attains the maximum ($\mu \approx 0.5$).

When μ_0 and μ_1 are separated further, the winter cell and the summer cell are separated at the confluent point where $u = 0$ and $v = 0$. This point now is not at the same latitude as the ITCZ nor the warmest place. Figure A4 displays the solution for $\mu_0 = 0.3$, $\mu_1 = 0.1$. The contour of the streamfunction is shown in Fig. A4a. The winter cell starts at the confluent point, which is poleward of $\mu_0 = 0.3$ ($\mu \approx 0.37$), and extends across the equator to the winter hemisphere. The strength is twice that in Fig. 14a. The summer cell is poleward of the confluent point up to the latitude where the equilibrium zonal attains maximum (see Fig. A4b). Figure A4b shows the zonal wind at the top. There is an interesting new feature in that zonal wind is discontinuous inside the circulation region (at $\mu_1 = 0.1$). It seems possible that there are multiple angular momentum conservation regions. Figure A4c shows the contour of the temperature (solid lines) and the equilibrium temperature (dashed lines). The horizontal profile of the temperature has a slight curvature since the meridional circulation is very strong.

REFERENCES

Batchelor, G. K., 1956: On steady laminar flow with closed streamlines at large Reynolds number. *J. Fluid Mech.*, **1,** 177–190.

Cane, M. A., and E. S. Sarachik, 1989: *Course on Ocean–Atmosphere Interactions in the Tropics*. United Nations Development Organization, International Center for Science and Technology, 288 pp.

Charney, J. G., 1973: Planetary fluid dynamics. *Dynamic Meteorology,* P. Morel, Ed., D. Reidel, 97–351.

Emanuel, K. A., J. D. Neeling, and C. S. Bretherton, 1994: On large-scale circulation in convecting atmosphere. *Quart. J. Roy. Meteor. Soc.*, **120,** 1111–1143.

Fang, M., and K. K. Tung, 1994: Solution to the Charney problem of viscous symmetric circulation. *J. Atmos. Sci.*, **51,** 1261–1272.

Graham, N. E., and T. P. Barnet, 1987: Sea surface temperature, surface wind divergence, and convection over tropical oceans. *Science,* **238,** 657–659.

Held, I. M., and A. Y. Hou, 1980: Nonlinear axially symmetric circulations in a nearly inviscid atmosphere. *J. Atmos. Sci.*, **37,** 515–533.

Hou, A. Y., and R. S. Lindzen, 1992: The influence of concentrated heating on the Hadley circulation. *J. Atmos. Sci.*, **49,** 1233–1241.

Lindzen, R. S., and A. Y. Hou, 1988: Hadley circulation for zonally averaged heating centered off the equator. *J. Atmos. Sci.*, **45,** 2416–2427.

Numaguti, A., 1993: Dynamics and energy balance of the Hadley circulation and the tropical precipitation zones: Significance of the distribution of evaporation. *J. Atmos. Sci.*, **50,** 1874–1887.

Oort, A. H., 1983: Global atmospheric circulation statistics, 1958–1973. NOAA Prof. Paper 14. U.S. Govt. Printing Office, 180 pp.

Plumb, R. A., and A. Y. Hou, 1992: The response of a zonally symmetric atmosphere to subtropical thermal forcing: Threshold behavior. *J. Atmos. Sci.*, **49,** 1790–1799.

Riehl, H., and J. S. Malkus, 1958: On the heat balance of the equatorial trough zone. *Geophis.*, **6,** 503–538.

Sarachik, E. S., 1978: Tropical sea surface temperature: An interactive one-dimensional atmosphere–ocean model. *Dyn. Atmos. Oceans,* **2,** 455–469.

Satoh, M., 1994: Hadley circulation in radiative-convective equilibrium in an axially symmetric atmosphere. *J. Atmos. Sci.*, **51,** 1947–1968.

——, and Y.-Y. Hayashi, 1992: Simple cumulus models in one-dimensional radiative convective equilibrium problems. *J. Atmos. Sci.*, **49,** 1202–1220.

Schneider, E. K., 1977: Axially symmetric steady-state models of the basic state for instability and climate studies. Part II: Nonlinear calculations. *J. Atmos. Sci.*, **34,** 280–296.

——, 1983: Martian great storms: Interpretive axially symmetric models. *Icarus,* **55,** 302–331.

——, and R. S. Lindzen, 1977: Axially symmetric steady-state models of the basic state for instability and climate studies. Part I: Linear calculations. *J. Atmos. Sci.*, **34,** 263–279.

Stevens, D. E., 1983: On symmetric stability and instability of zonal mean flows near the equator. *J. Atmos. Sci.*, **40,** 882–893.

Tung, K. K., 1986: Nongeostrophic theory of zonally averaged circulation. Part I: Formulation. *J. Atmos. Sci.*, **43,** 2600–2618.

Yanai, M., S. Esbensen, and J.-H. Chu, 1973: Determination of bulk properties of tropical cloud clusters from large-scale heat and moisture budgets. *J. Atmos. Sci.*, **30,** 611–627.